ANNULAR JETS

by

Michael Stewart Borgas

B.Sc.(Hons.), University of Adelaide.

Thesis submitted for the Degree of

Master of Science

in the

University of Adelaide

Department of Applied Mathematics.

September 1982.

TABLE OF CONTENTS

SUMMARY

In this thesis annular jets, falling vertically (when gravity is included), are considered. Thus in any horizontal plane the jet lies between two concentric circles. The three main jet parameters examined are surface tension, jet thickness and a pressure difference across the annulus. Various types of dynamic behaviour are also considered, including formation of jets from nozzles and stability of jets.

Techniques are developed where the behaviour of such jets may be described mathematically, and solutions for a wide spectrum of jet parameters presented.

SIGNED STATEMENT

I hereby declare that this thesis contains no material which has been accepted for the award of any other degree or diploma in any University and, to the best of my knowledge, it contains no material previously published by any other person, except where due reference is made in the text of the thesis.

...

M. S. BORGAS.

ACKNOWLEDGEMENTS

I would like to thank my supervisor, Professor E.O. Tuck, for his advice and guidance in completing this thesis.

I would also like to thank Ms. E. Henderson for her excellent typing.

The work for this thesis was carried out from January 1982 to September 1982, during which time I was financed by an Adelaide University Research Grant.

INTRODUCTION

This thesis describes research on three aspects of the behaviour of axisymmetric annular jets. These are categorized as follows:

(i) Formation of a jet from a nozzle (Chapter 1),

(ii) Computation of the free surfaces for a *free* slender jet (Chapter 2),

(iii) Stability of an annular column (Chapter 3).

Each of these topics, though distinctly different in so far as the analysis is concerned, is unified by the practical considerations of real annular jets. Such jets have a wide spectrum of applications, ranging from irrigation sprinklers to "shrouding" of nuclear reactors. However, discussion of these and other applications is omitted from this thesis.

In general, throughout this thesis we examine irrotational flows of an ideal fluid, usually thought of as water. However, at times, the influence of surface tension on the free surfaces of the jet are included. This allows us to use potential theory for the mathematical formulation of the problem, that is, we aim to find the velocity potential in the region of flow, together with the free boundaries enclosing this region. Although, in general, the problem thus formulated cannot be solved exactly, the following three chapters introduce approximations that facilitate the solution task.

Problem (i) is composed of a flow with mixed rigid boundaries (pipes) and free boundaries; this leads to a boundary-value problem

with mixed normal and tangential (derivative) boundary conditions. For the case of a slender nozzle this problem may be linearized in the "transition" region, close to the pipe orifice, where the flow is necessarily *not slender*. The free jet downstream from the transition region depends on one parameter, κ, obtained by solving the "transition flow" problem. This parameter is related to the "initial" slope of the slender jet discharging from the orifice, which if known permits the free boundaries to be computed (cf. Chapter 2).

For a certain class of nozzle (those with the orifice in a horizontal plane), the linearized problem can be solved using eigenfunction expansions. The resultant algebraic system is solved numerically on the computer, and results for κ presented.

Problem (ii) in exact form is simplified by making use of slenderness approximations. That is, we seek asymptotic expansions for the velocity potential and the free boundaries. This leads to a non-linear ordinary differential equation to solve, which is accomplished using a standard numerical algorithm (see page 28.). Solutions for a variety of parameters (related to jet thickness, surface tension and a pressure difference across the annulus) are investigated, primarily discussed with respect to a geometric property of annular jets, the "collapse-length". This length is the distance from the source of the jet, where the "initial" conditions are applied, to where the inner free surface coalesces and the jet becomes a solid cylinder.

Further work in Chapter 2 discusses *thin* annular jets, where analytic solutions are found when these jets are also slender. Theories exist in the literature for such thin (non-slender)

annular jets, or "water-bells" as they are sometimes known, and comparisons of the results are made. Our more-rigorous techniques (formal asymptotic analysis) provide a better understanding than some of these theories.

Chapter 3, discussing problem (iii), uses an infinitesimal wave-like theory to aid in the understanding of how disturbances grow in time (temporally), on the surfaces of annular columns. That is, a periodic time dependent perturbation to the free surface is considered, and terms to first-order in amplitude are retained throughout the analysis. We obtain from this analysis a dispersion relationship and an amplification relationship, which describe respectively, the growth rate in time (as a function of disturbance wavelength) and the interaction of the disturbances on either free surface. The analysis is not entirely "new", however a different interpretation is given to these "old" results, augmented by some new results. This appears to lead to more satisfactory conclusions than have appeared in the literature. In particular explicit physical explanation is given for the case of the "break-up" of annular columns, where the inner air core is a small perturbation to the jet as a whole.

CHAPTER 1

ANNULAR NOZZLES

1. INTRODUCTION

It was recently shown, Tuck (1982), that the free surfaces $r = a(z), b(z)$ of a slender free annular jet may be computed by solving a non-linear ordinary differential equation, as an initial-value problem. This task is relatively straightforward, and such solutions may be considered almost analytic, in comparison with the enormous numerical task of computing the free surfaces of slender streams with arbitrary cross sections. The latter problem has been tackled by Geer and Strikwerda (1981).

The emphasis of this chapter is to quantify the initial parameters of the free annular jet, namely the inner and outer radii, and one of the initial longitudinal slopes, given that the jet issues from a slender, annular, pipe. We define a nozzle as the abrupt end of a pipe from where a jet may issue. The "pipe flow" is readily computed, to leading order in slenderness, by conservation of mass at each z-section along the pipe. This gives the velocity in the z-direction and also the direction of flow at the inner and outer pipe walls.

It is important to note, as was indicated in Tuck (1982), that the initial free jet flow is not just an extrapolation of the emerging pipe flow. The reason for this is that, in the pipe flow, there are four parameters at each section, namely the two pipe radii and two longitudinal slopes of the pipe walls. If these are all independently specified, the longitudinal velocity $U(z)$ is determined

at each section, by conservation of mass. However, once the jet is formed, the velocity is specified at each z section by the condition that the free surface pressure be atmospheric, and conservation of mass then requires that the inner and outer radii and the corresponding slopes are no longer independent. Thus a jet cannot be thought of as an extension of the pipe. Tuck (1982) resolves this paradox by noticing there must be a region of flow, the nozzle or transition region, which is non-slender.

The transition flow problem is far more difficult to analyze than either the slender pipe flow or the slender jet flow. However the region of this flow is confined to very near the actual termination of the pipe and is to leading order independent of the local pipe curvature at the nozzle. Thus, we may assume that the pipe geometry varies linearly with z, and the velocity, $U_0 = U(0)$ say, dominates the flow, and is constant in the transition region. Using these assumptions Tuck (1982) formulated the axisymmetric boundary-value problem and gave the matching procedure needed to determine the initial parameters of the free jet. In particular the initial radii of the jet are equal to the nozzle radii, and the primary task is to determine the initial jet *slopes*, given the nozzle slopes.

The equivalent two-dimensional class of problems has been studied extensively, Geer and Keller (1979) giving comprehensive techniques and matching procedures to solve a wide range of problems. However the limiting case of thin annular jets, which may be approximated by the analogous two dimensional problem, and, for which Tuck (1982) gives the required matching formulae for the initial parameters, does not seem to be included in Geer and Keller results.

2. EQUATIONS FOR INITIAL SLOPE

The basic problem we address ourselves to is the canonical "potential" problem defined in Tuck (1982). We also adopt the notation from this publication, namely ψ is the canonical potential, a_0, b_0 the inner and outer radii respectively and 0_- denotes the pipe part of the transition zone while 0_+ denotes the jet part of the transition zone. Thus $a'(0_-)$ is the slope of the inner pipe and $b'(0_-)$ the slope of the outer pipe. The output parameter that we wish to compute is the jet's initial inner slope $a'(0_+)$. The most general problem also allows the nozzle to be offset, that is, the outer pipe terminates at $z=0$, say, and the inner pipe at $z = L$. We shall initially confine our attention to the case $L=0$; thus the pipe ends at $z=0$, at both sides of the annulus, and the free jet begins.

The boundary-value problem for ψ in this case is the following. We solve the axisymmetric Laplace equation,

$$\frac{\partial^2\psi}{\partial r^2} + \frac{1}{r}\frac{\partial\psi}{\partial r} + \frac{\partial^2\psi}{\partial z^2} = 0, \qquad (2.1)$$

in the pipe and jet $(a_0 \leqslant r \leqslant b_0)$, together with the boundary conditions,

$$\psi_r = 0 \quad \text{on} \quad r = a_0, b_0 \quad z \leqslant 0, \qquad (2.2)$$

and

$$\psi_z = z \quad \text{on} \quad r = a_0, b_0 \quad z \geqslant 0. \qquad (2.3)$$

Once this problem is solved for ψ, a parameter κ is defined by

$$(b_0 - a_0)\kappa = \lim_{z\to\infty} \psi_r(a_0, z) \ . \qquad (2.4)$$

It is of interest to note that (2.1) - (2.3) define ψ only up to an arbitrary constant; however, in view of the differentiation in (2.4), this non-uniqueness is irrelevant, and it is convenient to impose the artificial condition $\psi \to 0$ as $z \to -\infty$. The solution of (2.1) - (2.3) together with this added condition is unique.

The matching equation, with (2.4) as the definition of κ, is given by Tuck (1982) (p. 15 Eqn. (5.11)) and is

$$a'(0_+) = a'(0_-) + (b_0-a_0)\kappa\left\{\frac{2}{b_0^2-a_0^2}(b_0b'(0_-)-a_0a'(0_-)) - \frac{g}{U_0^2}\right\}, \quad (2.5)$$

where g is the usual gravitational constant and U_0 the dominant velocity component of the stream. The problem for κ is independent of the nozzle slopes $a'(0_-)$ and $b'(0_-)$ and can be further simplified if we scale all lengths with respect to a_0 and put $\beta = \frac{b_0}{a_0}$ as the new geometrical parameter. The new "non-dimensional" canonical potential, scaled with respect to a_0^2, satisfies the following boundary-value problem, namely the axisymmetric Laplace equation,

$$\frac{\partial^2\psi}{\partial r^2} + \frac{1}{r}\frac{\partial\psi}{\partial r} + \frac{\partial^2\psi}{\partial z^2} = 0 \quad \text{for} \quad 1 < r < \beta, \quad (2.6)$$

with boundary conditions

$$\psi_r = 0 \quad \text{on} \quad r = 1,\beta \quad \text{and} \quad z \leqslant 0, \quad (2.7)$$

and

$$\psi_z = z \quad \text{on} \quad r = 1,\beta \quad \text{and} \quad z \geqslant 0. \quad (2.8)$$

κ is now a function of β only (and L also in the general case) and is given by the revised form of (2.4) as

$$(\beta-1)\kappa = \lim_{z\to\infty} \psi_r(1,z), \quad (2.9)$$

together with the new matching equation,

$$a'(0_+) = a'(0_-) + (\beta-1)\kappa\left\{\frac{2}{\beta^2-1}(\beta b'(0_-)-a'(0_-)) - \frac{ga_0}{U_0^2}\right\} . \quad (2.10)$$

Conservation of mass in the free jet, $z \geqslant 0$, leads to the following equation

$$\beta b'(0_+) = a'(0_+) - \frac{ga_0}{2U_0^2}(\beta^2-1) , \quad (2.11)$$

which determines the *outer* initial free surface slope, once the inner slope $a'(0_+)$ is found from (2.10).

3. SEPARATION OF VARIABLES EQUATIONS

To solve the boundary-value problem (2.6) - (2.8), we need to use a numerical approach. Because of the geometry involved it is logical to use a separation of variables technique, and this approach is outlined below.

In the upstream region, $z \leqslant 0$, subject to the boundary condition (2.7), we use the eigenfunction expansion

$$\psi(r,z) = \sum_{n=1}^{\infty} A_n U_0(\alpha_n r) e^{\alpha_n z} , \quad (3.1)$$

for the canonical potential ψ. In (3.1) $U_0(\alpha_n r)$ is a cylinder function defined by

$$U_0(\alpha_n r) = Y_1(\alpha_n)J_0(\alpha_n r) - J_1(\alpha_n)Y_0(\alpha_n r) , \quad (3.2)$$

where $J_0(r), Y_0(r)$ are the zeroth order Bessel functions of the first and second kind respectively. Similarly $J_1(r), Y_1(r)$ are the first order Bessel functions. The form of (3.1) satisfies the axisymmetric Laplace equation and the eigenvalues, α_n, are computed by requiring

$$U_0'(\alpha_n) = U_0'(\alpha_n \beta) = 0 \ ,$$

which leads to the following equation,

$$U_1(\alpha_n \beta) = Y_1(\alpha_n)J_1(\alpha_n \beta) - J_1(\alpha_n)Y_1(\alpha_n \beta) = 0 \ . \qquad (3.3)$$

Thus (3.1) satisfies the boundary value problem for $z \leqslant 0$, but as yet, the coefficients A_n are unknown.

In the downstream region, $z \geqslant 0$, subject to the boundary condition (2.8), we use the eigenfunction expansion

$$\psi(r,z) = (\frac{1}{2}z^2 - \frac{1}{4}r^2) + B_0 \log r + A_0 + \sum_{n=1}^{\infty} B_n \mathcal{D}_0(\gamma_m r)e^{-\gamma_m z} \ . \qquad (3.4)$$

In this case the cylinder function $\mathcal{D}_0(\gamma_m r)$ is given by

$$\mathcal{D}_0(\gamma_m r) = Y_0(\gamma_m)J_0(\gamma_m r) - J_0(\gamma_m)Y_0(\gamma_m r) \qquad (3.5)$$

from which the boundary conditions

$$\mathcal{D}_0(\gamma_m) = \mathcal{D}_0(\gamma_m \beta) = 0$$

lead to

$$Y_0(\gamma_m)J_0(\gamma_m \beta) - J_0(\gamma_m)Y_0(\gamma_m \beta) = 0 \qquad (3.6)$$

for the determination of the eigenvalues γ_m. The remaining terms in (3.4) serve to make the boundary conditions for the cylinder function, $\mathcal{D}_0(\gamma_m r)$, homogeneous. The logarithm term contains the essential output quantity of this investigation, B_0, which is the only (non-constant) non-zero term at downstream infinity.

Equation (3.4) satisfies the boundary value problem for $z \geqslant 0$; however the coefficients B_n, as were the A_n, for $n=0,1,2,\ldots$ are as yet undetermined. To solve for these remaining unknowns we

require (3.1) and (3.4) and the corresponding z derivatives, to match at the mutual boundary $z=0$. This leads to the set of equations which must hold for all r in $1 \leqslant r \leqslant \beta$:

$$\sum_{n=1}^{\infty} A_n U_0(\alpha_n r) = -\frac{1}{4}r^2 + B_0 \log r + A_0 + \sum_{n=1}^{\infty} B_n \mathcal{D}_0(\gamma_n r) \qquad (3.7)$$

and

$$\sum_{n=1}^{\infty} \alpha_n A_n U_0(\alpha_n r) = -\sum_{n=1}^{\infty} \gamma_n B_n \mathcal{D}_0(\gamma_n r), \qquad (3.8)$$

These can, in principle, be solved for the unknown coefficients A_n, B_n for $n=0,1,2,\ldots$. No solution, however, in closed form, can be found to this set of equations.

4. NUMERICAL PROCEDURE

We first consider the problem of solving (3.3) and (3.6) for the eigenvalues α_n and γ_n respectively. For large α_n and γ_n asymptotic formulae, for these eigenvalues, are given in Abramowitz and Stegun (1970) (p. 374, Eqn. 9.5.28). These equations provide good initial iterates, for an iteration procedure to solve the non-linear equations (3.3) and (3.6). Using Newton's iteration rapid convergence to the correct root is found for β not too large. In the latter case the asymptotic formulae are not valid for the first few roots and an alternative means is required for providing initial guesses. Tables, again from Abramowitz and Stegun (1970) (p. 415) and linear interpolation are adequate for this purpose.

An initial attempt to solve the equations (3.7) and (3.8) was by the method of collocation. This, however, proved to be entirely unsatisfactory, due probably to the highly oscillatory nature of the Bessel functions in (3.1) and (3.4), for large eigenvalues. The

resulting matrices obtained by requiring equations (3.7) and (3.8) to be satisfied at N+1 points, and truncating the infinite series after N terms, are highly ill-conditioned, and unreliable results are obtained with any of the inversion packages tried.

The next attempt at solving equations (3.7) and (3.8) for the unknowns A_n, B_n (n=0,1,...) is to use the orthogonality of Cylinder functions. More precisely it will involve a hybrid method of solution, combining orthogonality and collocation to arrive at a consistent, and invertible, system of algebraic equations.

We first differentiate (3.7) and (3.8) with respect to r to arrive at the new equations

$$\sum_{n=1}^{\infty} \alpha_n A_n U_1(\alpha_n r) = \frac{1}{2}r - B_0/r + \sum_{n=1}^{\infty} \gamma_n B_n \mathcal{D}_1(\gamma_n r) \qquad (4.1)$$

and

$$\sum_{n=1}^{\infty} \alpha_n^2 A_n U_1(\alpha_n r) = -\sum_{n=1}^{\infty} \gamma_n^2 B_n \mathcal{D}_1(\gamma_n r) \ . \qquad (4.2)$$

The reason for considering equations (4.1) and (4.2) will become evident shortly. The cylinder functions $U_1(\alpha_n r)$ and $\mathcal{D}_1(\gamma_n r)$ are given by

$$U_1(\alpha_n r) = Y_1(\alpha_n)J_1(\alpha_n r) - J_1(\alpha_n)Y_1(\alpha_n r) \qquad (4.3)$$

and

$$\mathcal{D}_1(\gamma_n r) = Y_0(\gamma_n)J_1(\gamma_n r) - J_0(\gamma_n)Y_1(\gamma_n r). \qquad (4.4)$$

Now from Watson (1958) (p. 466) we get the following definite integrals

$$\int_1^{\beta} r\mathcal{D}_1(\gamma_n r)\mathcal{D}_1(\gamma_m r)dr = 0 \qquad \text{if } m \neq n$$

$$= \frac{1}{2}[\beta^2\mathcal{D}_1^2(\beta\gamma_n) - \mathcal{D}_1^2(\gamma_n)] \quad \text{if } n = m.$$

Thus, using this orthogonality relation, and also noting that

$$\int_1^\beta \mathcal{D}_1(\gamma_m r)dr = \left[-\frac{1}{\gamma_m}\mathcal{D}_0(\gamma_m r)\right]_1^\beta = 0,$$

we find that equations (4.1) and (4.2) become, after multiplying by $r\mathcal{D}_1(\gamma_m r)$ and integrating with respect to r,

$$\sum_{n=1}^{\infty} \alpha_n A_n \Lambda'_{mn} = \frac{1}{2}\Gamma'_m + \gamma_m B_m \frac{1}{2}(\beta^2\mathcal{D}_1^2(\gamma_m\beta) - \mathcal{D}_1^2(\gamma_m))$$

and

$$\sum_{n=1}^{\infty} \alpha_n A_n \Lambda'_{mn} = -\gamma_m^2 B_m \frac{1}{2}(\beta^2\mathcal{D}_1^2(\gamma_m\beta) - \mathcal{D}_1^2(\gamma_m))$$

where

$$\Lambda'_{mn} = \int_1^\beta r\mathcal{D}_1(\gamma_m r)U_1(\alpha_m r)dr$$

and

$$\Gamma'_m = \int_1^\beta r^2\mathcal{D}_1(\gamma_m r)dr ,$$

for $m=1,2,3,\ldots$. Furthermore, upon elimination of B_m, these equations reduce to give

$$\sum_{n=1}^{\infty} \alpha_n \left(1 + \frac{\alpha_n}{\gamma_m}\right)\Gamma'_{mn} A_n = \frac{1}{2}\Gamma'_m , \quad \text{for} \quad m=1,2,\ldots . \tag{4.5}$$

The integrals Λ'_{mn} and Γ'_m may be written in closed form as

$$\Lambda'_{mn} = \frac{\alpha_n}{\gamma_m^2-\alpha_n^2}\{\beta\mathcal{D}_1(\gamma_m\beta)U_0(\alpha_n\beta) - \mathcal{D}_1(\gamma_m)U_0(\alpha_n)\}$$

and

$$\Gamma'_m = \frac{2}{\gamma_m^2}\{\beta\mathcal{D}_1(\gamma_m\beta) - \mathcal{D}_1(\gamma_m)\} . \tag{4.6}$$

The algebraic system (4.5) may be written in a more compact form as

$$\Lambda\underset{\sim}{A} = \underset{\sim}{\Gamma}, \tag{4.7}$$

where

$$\Lambda = [\Lambda_{mn}] = [\alpha_n (1 + \frac{\alpha_n}{\gamma_m}) \Lambda'_{mn}] ,$$

$$\underset{\sim}{A} = [A_m]$$

and $\underset{\sim}{\Gamma} = [\Gamma_m] = [\frac{1}{2}\Gamma'_m]$, with Λ'_{mn} and Γ'_m as given in (4.6). This resultant form of algebraic equations illustrates that (4.1) and (4.2) are indeed the correct equations to study when applying this solution procedure. (4.7) is a consistent system to solve for the unknowns A_n, $n=1,2,\ldots$, and from these we determine the remaining unknowns.

The numerical procedure we adopt is to truncate the series in (4.5) and solve for the unknowns $A_n^{(N)}$ for $n=1,2,\ldots,N$. The superscript N indicates this solution is in some sense an approximation to the actual solution, A_n, we seek. The approximate problem we now solve can be expressed as

$$\Lambda^{(N)} \underset{\sim}{A}^{(N)} = \underset{\sim}{\Gamma}^{(N)} , \qquad (4.8)$$

where $\Lambda^{(N)}$ is an $N\times N$ matrix given by $[\Lambda_{mn}]$ for $m,n=1,2,\ldots,N$. $\underset{\sim}{A}^{(N)}$ is the $N\times 1$ solution vector and $\underset{\sim}{\Gamma}^{(N)}$ is an $N\times 1$ column vector given by $[\Gamma_m]$ for $m=1,2,\ldots,N$. Any standard package may be used to invert $\Lambda^{(N)}$ and thus obtain the solution $\underset{\sim}{A}^{(N)}$ to this system of equations.

This numerical procedure is satisfactory provided the approximate solution $\underset{\sim}{A}^{(N)}$ converges to a limit as $N \to \infty$. Naturally we require this limit to be bounded and we furthermore expect $A_n^{(N)} \to 0$ as $n,N \to \infty$. This latter condition is an a priori justification of the

truncation of the series (4.5) which results in this algebraic, solvable, system of equations. One further check on this numerical solution is the comparison of the limit $\beta \to 1$, or thin annular jet limit and we do this later on.

5. COMPUTING KAPPA

Having computed the coefficients A_n by orthogonality we now wish to compute κ. This requires solving for the unknowns A_0 and B_0. We note that the A_n's uniquely define the B_n's for $n > 1$. To do this we return to the method of collocation, specifically evaluating (3.7) at $r=1$ and $r=\beta$. The resulting equations are

$$A_0 = \frac{1}{4} + \sum_{n=1}^{\infty} A_n U_0(\alpha_n)$$

and

$$B_0 \log \beta + A_0 = \frac{1}{4}\beta^2 + \sum_{n=1}^{\infty} A_n U_0(\alpha_n \beta) \ .$$

Eliminating A_0 from these two equations gives

$$B_0 \log \beta = \frac{1}{4}(\beta^2-1) + \sum_{n=1}^{\infty} A_n \{U_0(\alpha_n \beta) - U_0(\alpha_n)\} \qquad (5.1)$$

and by virtue of the definition of κ we have

$$\kappa = (B_0 - \tfrac{1}{2})(\beta - 1)^{-1} \ . \qquad (5.2)$$

The corresponding approximate numerical results are given by the equations

$$B_0^{(N)} \log \beta = \frac{1}{4}(\beta^2-1) + \sum_{n=1}^{N} A_n^{(N)} \{U_0(\alpha_n \beta) - U_0(\alpha_n)\} \qquad (5.3)$$

and

$$\kappa^{(N)} = (B_0^{(N)} - \tfrac{1}{2})(\beta - 1)^{-1} . \qquad (5.4)$$

Equations (5.3) and (5.4), in conjunction with the method described in §4 for determining $\underset{\sim}{A}^{(N)}$, constitute a numerical

method for solving the problem. This method is relatively simple to program and makes little demand upon storage and time constraints.

6. NUMERICAL RESULTS

In practice the numerical scheme in §4 works satisfactorily. The matrices $\Lambda^{(N)}$ are well-conditioned and $\underset{\sim}{A}^{(N)}$ does indeed converge, in some sense, to a limit. We do find, however, that the last few terms of $\underset{\sim}{A}^{(N)}$, for example $A_{N-1}^{(N)}$, $A_N^{(N)}$ may be disproportionately large. Nevertheless, this numerical artefact has little to do with the convergence of $\kappa^{(N)}$, and tests, omitting or including these last few terms from (5.3), indicate little effect on the computation of $\kappa^{(N)}$. For the remainder of this section we discuss the numerical results for κ.

Although the convergence rates are relatively slow, with (for moderate β) decay of error terms like N^{-1}, the actual magnitude of errors is small enough to allow three-figure accuracy with $N \sim 20$. For β close to 1 convergence is more rapid and $N \sim 10$ suffices. Difficulties begin to occur when β becomes large, say greater than 20. The rate of convergence is even slower and good results need $N \sim 40$. It is interesting to note that this numerical scheme converges only for even N. If N is odd $\underset{\sim}{A}^{(2n+1)}$ is erratic as $n \to \infty$ and appears not to converge. In view of the satisfactory results when N is even this does not concern us overly much.

Results for κ, accurate to three figures, are plotted on Figure 1. The dashed line is a large β limit discussed next.

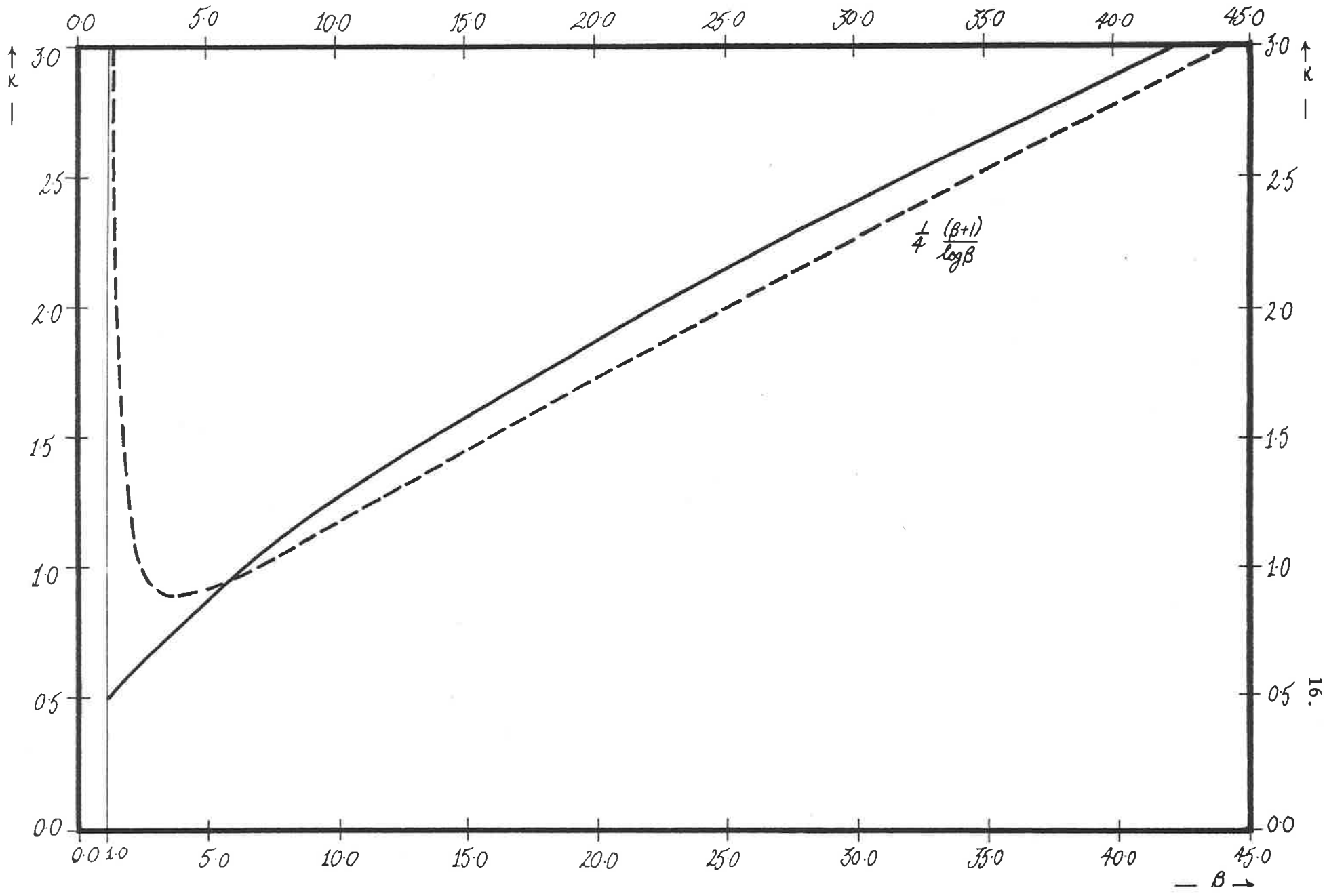

FIGURE 1.

$K(\beta)$ vs. β $(L \equiv 0{\cdot}0)$

7. LARGE β LIMIT

We consider equation (5.1). Numerical evidence suggests A_n is at most $O\{\log^2\beta\}$. Thus, neglecting terms of $O\{\log\beta\beta^{-1}\}$ from equation (5.1) and (5.2) we find that

$$\kappa(\beta) \sim \frac{\beta+1}{4 \log \beta} \quad \text{as} \quad \beta \to \infty . \tag{7.1}$$

We have as yet little insight into the physical interpretation of (7.1). However, if we consider the gravity-free case, $g=0$, we can verify the relative magnitudes of the large β limit intuitively.

From the matching equation (2.10), (7.1) implies that $a'(0_+)$ behaves like

$$a'(0_+) \sim \frac{\beta}{2 \log \beta} b'(0_-) \quad \text{as} \quad \beta \to \infty , \tag{7.2}$$

provided $b'(0_-)$ is non-zero, otherwise

$$a'(0_+) \sim - \frac{a'(0_-)}{2 \log \beta} \quad \text{as} \quad \beta \to \infty . \tag{7.3}$$

The behaviour of $b'(0_+)$ is given by equation (2.11) and either of (7.2), (7.3) depending on the value of $b'(0_-)$, thus we have

$$b'(0_+) \sim \frac{b'(0_-)}{2 \log \beta} \quad \text{as} \quad \beta \to \infty , \tag{7.4}$$

provided $b'(0_-)$ is non-zero, otherwise

$$b'(0_+) \sim - \frac{a'(0_-)}{2\beta \log \beta} \quad \text{as} \quad \beta \to \infty . \tag{7.5}$$

So clearly as β gets large the inner radius plays a decreasing role in the determination of the outer radius. The expected, straight cylinder, limit is verified by equations (7.4) and (7.5), giving $b'(0_+) \sim 0$. The sizes of the limits (7.2) and (7.3) can also be

rationalized. Supposing $b'(0_-)$ is non-zero firstly, then initially there is some small change in the outer radius of the jet . Correspondingly, because of the large outer radius relative to the inner radius, a more dramatic change occurs at the inner radius, in order to conserve mass. This is evident since $|a'(0_+)| \to \infty$ as $\beta \to \infty$ in this case. If $b'(0_-)$ is zero then it is not unreasonable to expect "continuity" of slope across the nozzle for the outer radius. In any respect, the slope $b'(0_+)$ is an order of magnitude less than when $b'(0_-)$ is non-zero. This is then reflected in the much slower change in the inner radius as indicated by equation (7.3).

Although we can explain the disparity of sizes of $a'(0_+)$ and $b'(0_+)$ using the concept of conservation of mass in a slender jet, more complicated concepts are needed to verify the actual limits given by (7.1). This work is not pursued at the moment.

8. OFFSET PIPES

When the pipe is offset at the nozzle, say the inner pipe ends at $L/2$ and the outer pipe at $-L/2$, there is a third region $-L/2 \leqslant z \leqslant L/2$ with mixed normal and longitudinal derivative boundary conditions. In the upstream region $z \leqslant -L/2$ we may still use the eigenfunction expansion given by (3.1). Similarly, downstream, $z \geqslant L/2$ we use (3.4). However, in the central region $-L/2 \leqslant z \leqslant L/2$ we require a new expansion. It is simple to verify that

$$\Psi(r,z) = \frac{1}{2}z^2 - \frac{1}{4}r^2 + \frac{1}{2}\log r + C_0 + \sum_{n=1}^{\infty} (C_n e^{\lambda_n z} + D_n e^{-\lambda_n z}) C_0(\lambda_n r) \qquad (8.1)$$

satisfies the required boundary conditions and the axisymmetric Laplace equation for $-L/2 \leqslant z \leqslant L/2$. $C_0(\lambda_n r)$ is the cylinder

function defined as

$$C_0(\lambda_n r) = Y_1(\lambda_n)J_0(\lambda_n r) - J_1(\lambda_n)Y_0(\lambda_n r), \qquad (8.2)$$

and the eigenvalues, λ_n, are roots of

$$C_0(\lambda_n \beta) = Y_1(\lambda_n)J_0(\lambda_n \beta) - J_1(\lambda_n)Y_0(\lambda_n \beta) = 0 . \qquad (8.3)$$

The unknowns $A_0, B_0, C_0, A_n, B_n, C_n, D_n$, $n=1,2,\ldots$ are now computed by matching (3.1) and (8.1) at $z = -L/2$, and (3.4) and (8.1) at $z = L/2$ much in the same way as is done in the $L=0$ case.

Preliminary attempts to solve this offset problem have failed. The matrices produced when using orthogonality are generally ill-conditioned and, if not, no convergence is evident after truncating the series at $N=20$. Of course, to use higher truncations becomes very expensive since the matrices are $2N \times 2N$ and a better numerical method is more desirable than lengthy computer runs. One case where good results are obtained by this method is the large L limit, (that is large relative to β-1), where κ rapidly tends to zero, implying continuity of the inner slope $a'(0_+) = a'(0_-)$. This is as expected. As of yet, we have not devised a means of computing $\kappa(\beta,L)$ for more general L and this remains as future work.

9. CONCLUSION

We have devised a satisfactory numerical method for computing $\kappa(\beta)$ for nozzles with no offset. Fortunately, this is common for practical nozzles and the remaining task of computing $\kappa(\beta,L)$, $L\neq 0$, is of lesser importance.

There is considerable evidence that $\kappa(\beta)$, computed in §5, is correct. We have the analytic two dimensional, comparison as $\beta \to 1$,

namely $\kappa \to 0.5$, which follows from Tuck (1982) (p. 14 (5.14)) with L=0. This is clearly seen to be the case. We also have the intuitive arguments of §6 justifying the large-β numerical results.

As a consequence of this work, practical problems involving slender pipes producing annular jets may be solved. For instance, given a pipe extending from $z = -\infty$ to $z=0$, say, and specified by $r = a(z), b(z)$ we may solve for the free annular jet produced. The initial ($z=0$) velocity of the jet is given by

$$U_0 = \frac{Q}{\pi(b_0^2 - a_0^2)} \quad , \tag{9.1}$$

where Q is the mass flux in the pipe and may be given by $\pi(b_\infty^2 - a_\infty^2)U_\infty$. The local nozzle slopes at $z=0$ are $b'(0)$, $a'(0)$ and, given $\beta = b_0/a_0$, we now know κ. Thus, the initial jet slopes are known, $a'(0_+)$ by (2.10), $b'(0_+)$ by (2.11). The free streamlines may now be computed as described in Tuck (1982).

CHAPTER 2

ANNULAR JETS WITH SURFACE TENSION

1. INTRODUCTION

Tuck (1982) gives an analysis of slender, annular, jets of water. The water is assumed to be an ideal fluid and also to be flowing irrotationally. Two features, namely surface tension forces and a finite pressure difference across the annulus, are not included in the analysis of Tuck. The former, surface tension, was assumed by Tuck to be negligible, and in this chapter we examine circumstances when this assumption is likely to be invalid. Not surprisingly, thin annular jets, sometimes called "water-bells" or annular sheets of water, depend predominantly on surface tension forces and also upon the previously mentioned pressure difference.

Literature on water bells dates back to Boussinesq (1869). More recently this area of research has been pursued by Lance and Perry (1953), Taylor (1959) and Hoffman, Takahashi and Monson (1980), the last of these also in the context of slender jets. In all of these publications, the authors assume that the annulus is sufficiently thin, so that radial variations across the annulus may be disregarded. In particular then, the velocity and shape of the water bell depend only on the longitudinal coordinate (or equivalently the arc-length), thus reducing the problem to an ordinary, though non-linear, differential equation for the shape of the stream. We shall see however that the thin jet limit is only formally correct when the surface tension forces (and pressure difference) are of comparable magnitude with $\rho\frac{U_0^2 h}{a_0}$, where a_0 is the initial inner radius, U_0 the initial velocity and h the annular thickness, that is the

difference between the inner and outer radii, which is supposed small. Indeed, if this assumption is not true, namely if these forces are of magnitude much greater than the annular"thickness"we propose "new" equations governing the jet's shape.

In the following sections we derive, and solve, the equations of motion for a thick, but slender annular jet. This analysis is much the same as Tuck's, though incorporating surface tension and pressure differences. Given the assumption of an ideal fluid, flowing irrotationally we seek the velocity potential and the boundaries as a solution. The solution of this non-linear, boundary-value problem, after slenderness approximations, can be reduced to the task of solving a non-linear ordinary differential equation, as an initial value problem. This is readily accomplished numerically. We then choose to examine the thin-jet limit via this differential equation, by letting the thickness tend to zero in the thick-jet problem.

For the moment we do not consider the capillary instability of these jets, a question which is intimately connected with surface tension, but rather the shape of the free boundaries. In particular we shall be concerned with the longitudinal length measured from the genesis of the jet to the point, if it exists, where the jet ceases to be an annulus and becomes a "solid" cylindrical jet. This length is sometimes called the collapse or convergence length. In the ideal fluid case, without surface tension and a pressure difference, as studied by Tuck (1980), the convergence length is a function of the initial ratio of surface radii and longitudinal surface slope. In particular there exists some such jets that fail to collapse.

Including surface tension alters this conclusion somewhat, and it appears that ultimately surface tension dominates and causes the jets to collapse, regardless of the initial conditions.

The inclusion of the pressure jump across the annulus is analogous to having a finite cavitation number in the theory of cavities (see for example Gilbarg (1960)). Formally however, to use the slender flow approximation this pressure can only be of the order of $\rho \frac{U_0^2 h}{a_0}$ or less, that is to say small when compared to the square of the jet velocity. The added feature of the pressure jump raises an important question, namely whether this pressure jump is specified *a priori*, and thus may take arbitrary, albeit small, values. Alternatively is there some physical constraint that determines a unique pressure difference for a given jet? Such questions are likely to be related to the stability of these annular jets, and unsteady evolution of such jets. For the moment, we treat p, the pressure difference, as an input parameter and proceed to solve for the free jet surfaces.

2. EQUATION FOR THICK, SLENDER ANNULAR JETS

The notation we adopt is taken from Tuck (1982), namely we put ϕ equal to the total velocity potential in the jet and have $r = a(z), b(z)$ as the inner and outer radii of the free jet. Under the assumption of slenderness Tuck (1982) gives the following equations for Φ, the perturbation potential,

$$\Phi_{rr} + \frac{1}{r}\Phi_r = -U'(z), \quad \text{for} \quad z \geqslant 0, \; a < r < b, \tag{2.1}$$

where $U(z)$ is the leading order velocity in the jet. The kinematic boundary conditions (no normal flow) are approximated by

$$\Phi_r = a'(z)U(z) \qquad z \geqslant 0,\ r = a(z) \qquad (2.2)$$

and

$$\Phi_r = b'(z)U(z) \qquad z \geqslant 0,\ r = b(z)\ . \qquad (2.3)$$

The dynamical boundary condition (constant pressure on the free surfaces) given by Tuck (1982) are augmented by two additional terms, namely the pressure jump p, and the contribution to pressure on the free surface by uniform tension T. The resultant equations in exact form are,

$$\tfrac{1}{2}\phi_z^2 + \tfrac{1}{2}\phi_r^2 - gz + \frac{p}{\rho} + \frac{P(r,z)}{\rho} = C \qquad \text{on } r = a(z), \qquad (2.4)$$

together with

$$\tfrac{1}{2}\phi_z^2 + \tfrac{1}{2}\phi_r^2 - gz + \frac{P(r,z)}{\rho} = C \qquad \text{on } r = b(z), \qquad (2.5)$$

where C is a constant. $P(r,z)$ is the surface tension pressure, given by

$$P(r,z) = T\left(\frac{1}{R_1} + \frac{1}{R_2}\right), \qquad (2.6)$$

where R_1 is the radius of curvature at (r,z) in the horizontal (z = constant) plane and R_2 the radius of curvature in the vertical (θ = constant) plane. We now wish to make the appropriate slender flow approximations to (2.4) and (2.5). The existence of a leading order velocity $U(z)$ requires the cross flow to be small, which can only occur when $\frac{P(r,z)}{\rho} \ll \frac{1}{2}U^2(z)$ and $\frac{p}{\rho} \ll \frac{1}{2}U^2(z)$ for all $z \geqslant 0$. Provided these inequalities are true we can make the normal slender flow assumptions and furthermore must have $R_2 \gg R_1$. Intuitively these inequalities say that a slender annular jet cannot sustain a *large* pressure difference across the annulus, and remain

slender. Similarly, for large values of the tension T, the stream will tend to have large curvature R_1, however for typical parameters, in practical situations, T is sufficiently small numerically. Given that we have a slender jet, we may approximate (2.4) and (2.5) as follows. Equation (2.4) reduces to

$$U(z)\Phi_z + \frac{1}{2}\Phi_r^2 - \frac{T}{\rho a(z)}\frac{1}{} + \frac{p}{\rho} = C - \frac{1}{2}U_0^2 \quad \text{on} \quad r = a(z), \qquad (2.7)$$

and (2.5) becomes

$$U(z)\Phi_z + \frac{1}{2}\Phi_r^2 + \frac{T}{\rho}\frac{1}{b(z)} = C - \frac{1}{2}U_0^2 \quad \text{on} \quad r = b(z)\ . \qquad (2.8)$$

The leading order equations from (2.4) and (2.5) give

$$U(z) = (U_0^2 + gz)^{\frac{1}{2}}, \quad z \geqslant 0. \qquad (2.9)$$

It is important to note the difference in sign of the radius of curvature, R_1, on $r = a(z)$ and $r = b(z)$. This is because one surface is convex and the other concave with respect to the fluid-air interface. For our purposes it is unnecessary to evaluate the constant C, but in principal it can be evaluated as the left hand side of (2.7) at $z = 0$. U_0 is the velocity of projection of the jet at the $z = 0$ section, and g the acceleration due to gravity. We use the notation $a_0 = a(0)$ and $b_0 = b(0)$ to denote the initial radii of the free jet surfaces.

The boundary value problem we have to solve is (2.1) subject to the conditions (2.2), (2.3) and (2.7), (2.8). We next consider the solution of this system.

3. SOLUTION OF THE BOUNDARY VALUE PROBLEM

Equation (2.1) has the general solution

$$\Phi(r,z) = \lambda'(z)\log r + \mu'(z) - \frac{1}{2}r^2U'(z)\ , \qquad (3.1)$$

involving two unknown functions of z, denoted by $\lambda'(z)$ and $\mu'(z)$, where the dash denotes differentiation with respect to z. These functions are determined by satisfying the four boundary conditions (2,2), (2.3) and (2.7), (2.8), remembering that both boundaries are also unknown functions of z. The boundary conditions (2.2) and (2.3) require, as in Tuck (1982), that

$$\lambda(z) = \tfrac{1}{2}U(z)a^2(z), \qquad \text{for} \quad z \geqslant 0, \tag{3.2}$$

and also that

$$\tfrac{1}{2}U(z)[b^2(z)-a^2(z)] = C_0, \quad \text{for} \quad z \geqslant 0, \tag{3.3}$$

where C_0 is a constant determined by the initial conditions. (3.3) is the statement of conservation of mass in the jet, since the area of cross section of the jet is proportional to the difference in the square of the radii. The further equations to close the system are obtained from the dynamic conditions (2.7) and (2.8). Eliminating the unknown $\mu'(z)$ we find,

$$\lambda''(z) = \frac{CU''(z) - U^2(b'^2-a'^2) - \frac{2T}{\rho}(\frac{1}{a}+\frac{1}{b}) + \frac{2p}{\rho}}{2U \log (\frac{b}{a})}, \tag{3.4}$$

which together with (3.2) and (3.3) constitutes a quasi 3rd order non-linear ordinary differential equation for determining $\lambda(z)$, thus $a(z)$ and $b(z)$. The third order character is due to the constant C_0 in (3.3). Analytic solution of this system is out of the question, though it is straightforward to solve it numerically. It is convenient to non dimensionalize the equations, and we choose to scale vertical lengths, the z direction, with respect to $\frac{U_0^2}{g}$.

We scale radial lengths with respect to a_0, velocities with respect to U_0 and pressure with respect to ρU_0^2. The equations become

$$U(z) = (1 + 2z)^{\frac{1}{2}}, \tag{3.5}$$

$$\frac{1}{2}U(z)(b^2-a^2) = \frac{1}{2}(\beta^2-1), \tag{3.6}$$

and

$$\lambda''(z) = \frac{\frac{1}{2}(\beta^2-1)U'' - U(b'^2-a'^2) - \kappa(\frac{1}{a}+\frac{1}{b}) + \Delta}{2U \log(\frac{b}{a})}, \tag{3.7}$$

where the constants κ, Δ and β are given by

$$\kappa = \frac{2TU_0^2}{g^2\rho a_0^3}, \tag{3.8}$$

$$\Delta = \frac{2pU_0^2}{g^2\rho a_0^2},$$

and

$$\beta = b_0/a_0. \tag{3.9}$$

The "initial" conditions for the jet, that is, the parameters at the $z = 0$ cross section are $a(0) = 1$, $b(0) = \beta$ and $a'(0) = \sigma = \frac{a_0' g a_0}{U_0^2}$ where a_0' is the specified, dimensional, slope of the free surface at $z = 0$. The parameters κ and Δ, although arbitrary, are always small for slender jets. The non-dimensional parameter κ is a measure of the surface tension, and is related to more standard non-dimensional parameters, the Weber number W_e and the Froude number F_r, by

$$\kappa = \frac{F_r^4}{W_e}. \tag{3.10}$$

To solve the equation we begin at $z = 0.0$, with the aforementioned initial conditions and compute numerical approximations

to $\lambda(z_n)$, where $z_n = n(\Delta z)$, using the Runge-Kutta-Nyström algorithm (see Kreyszig, 1979, p. 802). This method is accurate to fourth order with respect to the increment (Δz). In our computations the collapse length is the primary output, and to ensure accuracy, the increment Δz is reduced as the inner radius approaches zero. In all our computations $\Delta z = 0.001$ gives sufficient accuracy.

4. COMPUTED RESULTS AND DISCUSSION

In Figure 1 we present actual jet shape profiles for thin jets, $\beta = 1.1$, and thick jets, $\beta = 2.0$. In each case two different values of the surface tension parameter κ were chosen. Qualitatively the shape of a jet influenced by surface tension is much the same as ideal jets discussed by Tuck (1982). The fundamental difference is quantitative, and the influence of surface tension is to reduce the collapse length Z_c. Indeed as we shall see surface tension may in fact cause some jets to have a finite Z_c value where otherwise, for the $\kappa = 0.0$ case, they do not collapse. The influence of surface tension is illustrated in Figure 2. The parameter space explored is the κ-β space, with reference to the collapse length Z_c. It is clear that, in the thick jet limit, $\beta \to \infty$, the role of surface tension is negligible. This is not so for thin jets, $\beta \to 1$, and it is apparent that only a very small value of κ is needed to cause the jet to collapse, whereas $\kappa = 0$ gives $Z_c \to \infty$. In Figure 3 we examine the Δ-β parameter space, again with respect to Z_c. In this case we can have Δ both positive, and negative. A negative value of Δ indicates an over-pressure, where the exterior pressure, presumably atmospheric, is greater than the

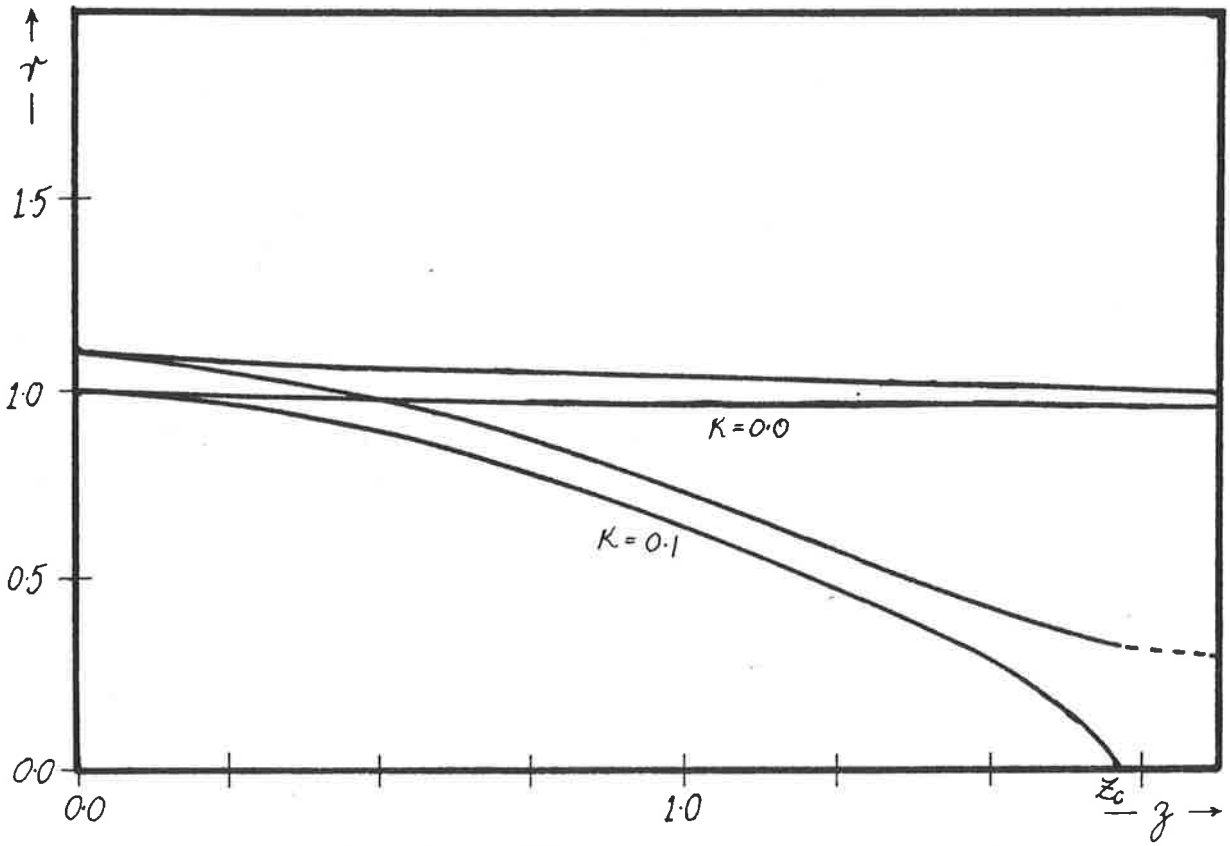

Annular Jets ($\Delta = 0{\cdot}0, \beta = 1{\cdot}1, \sigma = 0{\cdot}0$)

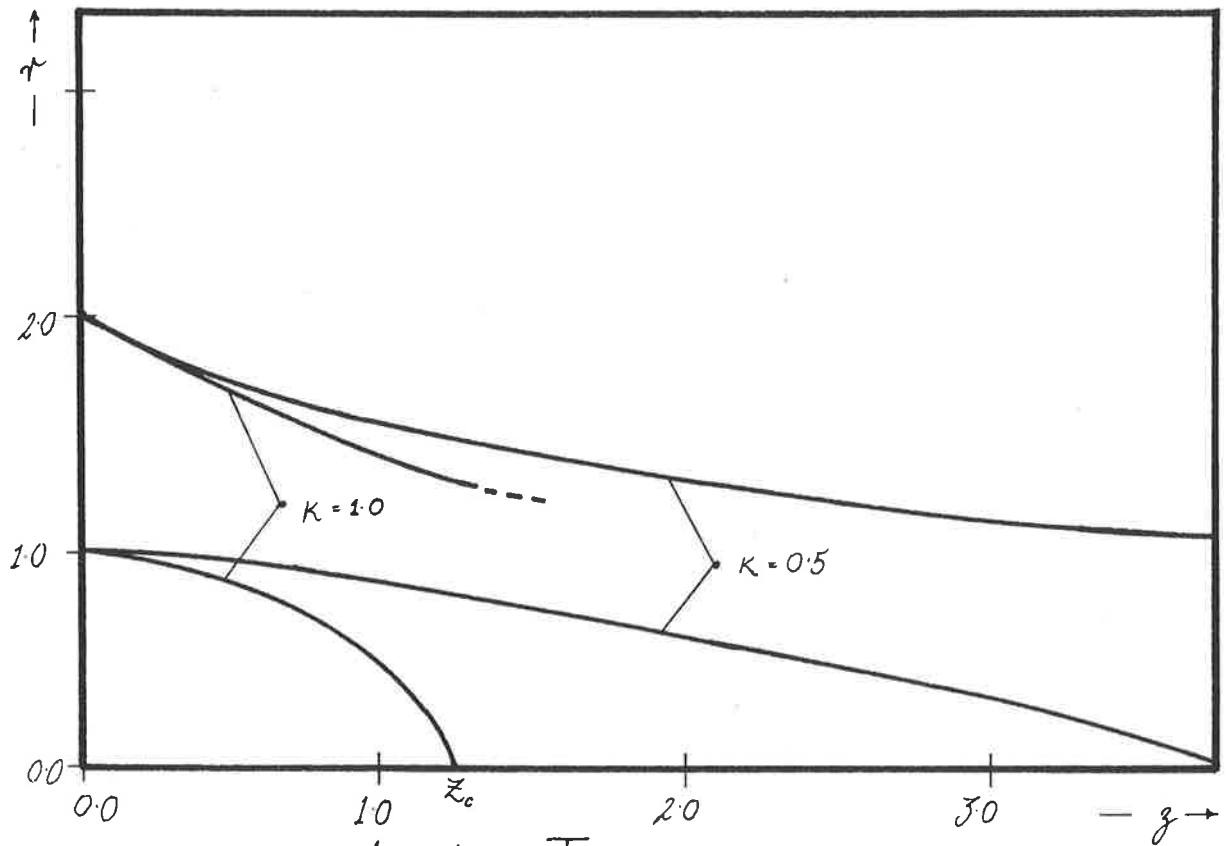

Annular Jets ($\Delta = 0{\cdot}0, \beta = 2{\cdot}0, \sigma = 0{\cdot}0$)

FIGURE 1.

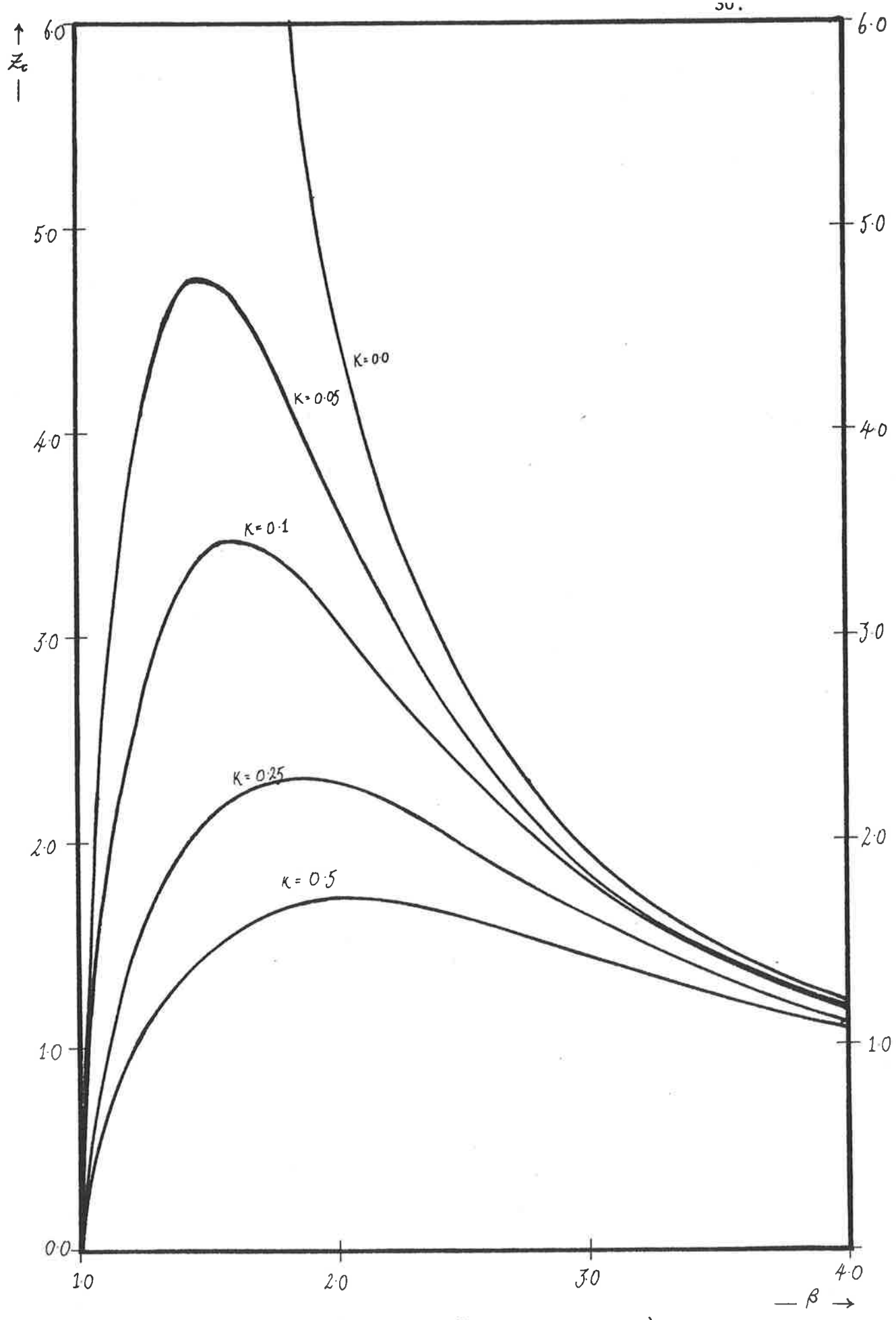

Z_c vs. β ($\Delta = 0{\cdot}0, \sigma = 0{\cdot}0$)

FIGURE 2.

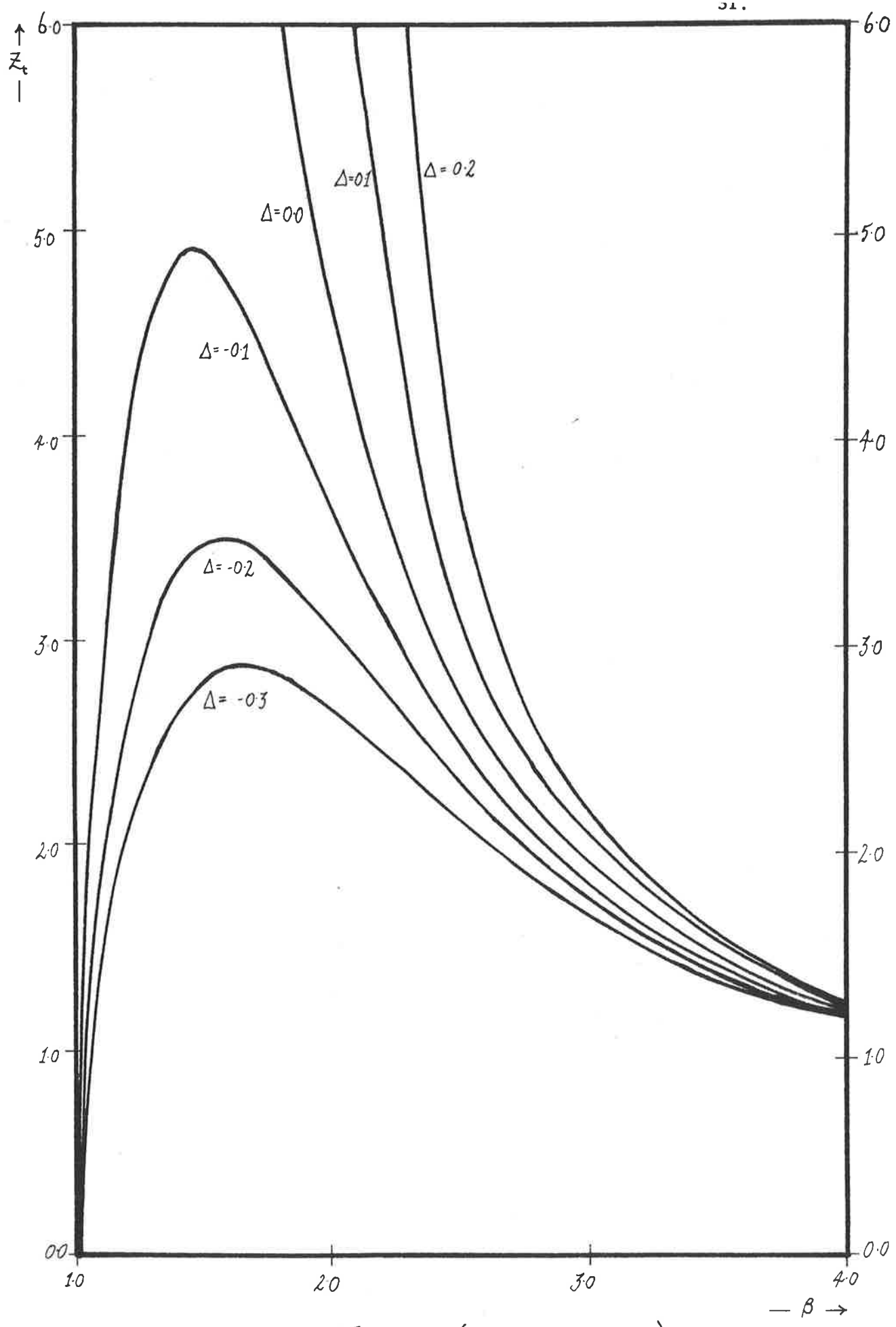

Z_c vs. β ($K = 0{\cdot}0$, $\sigma = 0{\cdot}0$)

FIGURE 3.

pressure in the hollow region of the jet. A positive Δ similarly indicates an underpressure. At once we note the similarity, qualitatively, of Figures 2 and 3. This is no doubt due to the roughly equivalent nature of the forces involved, that is, both acting normally to the annular surface. It would seem an over-pressure results in the jet always collapsing and this is perhaps not surprising. As the pressure difference is increased, ultimately becoming an under-pressure, the jet is more reluctant to collapse. Once again thin jets are most sensitive to the Δ parameter, thick jets insensitive. To compare the pressure-surface tension interaction Figure 4 presents results for the collapse distance in the κ-Δ parameter space. This shows that jets with an under-pressure will not collapse even with surface tension, unless κ is sufficiently large. This behaviour is investigated for thin jets in Figure 4, having $\beta = 1.1$. The corresponding results for a thick jet, $\beta = 2.0$ are given in Figure 5. We draw similar conclusions for thick jets. The most significant difference is due to the insensitivity of thicker jets to both surface tension and pressure forces. This results in Z_c generally being greater and the less rapid growth of Z_c as Δ increases. The final two figures, Figure 6 and Figure 7 consider the effect of initial slope, parameterised by σ. From Figure 6 we see that jets initially directed outward, $\sigma > 0$, will generally collapse, even for relatively small values of κ. The same is true for Figure 7, this time however with reference to the pressure jump. For over-pressures, jets will ultimately collapse even with $\sigma > 0$. For underpressures, however, it may be that σ need be less than zero, that is, the jet is initially directed in, for collapse to occur.

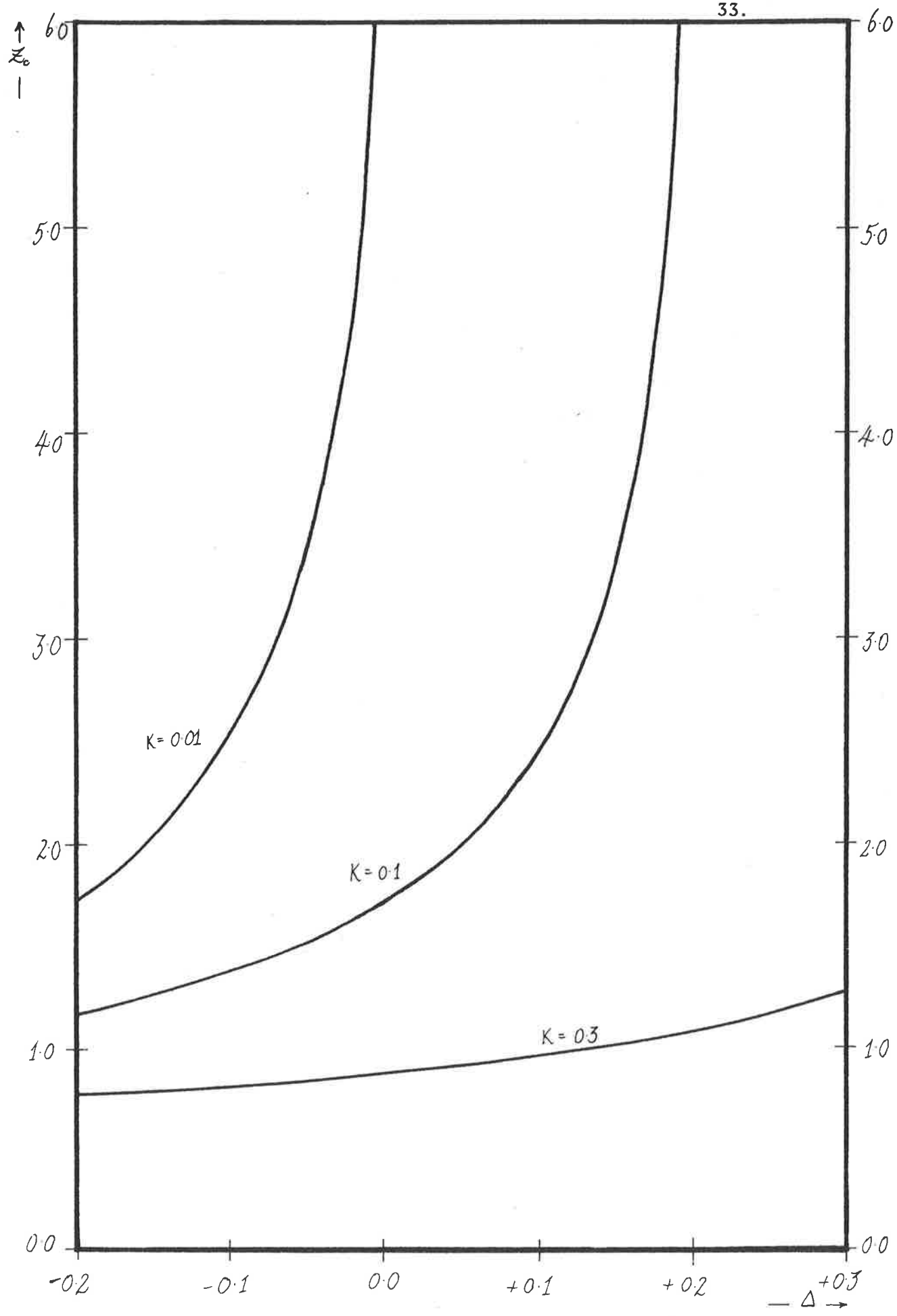

Z_c vs. Δ ($\beta = 1{\cdot}1$, $\sigma = 0{\cdot}0$)

FIGURE 4.

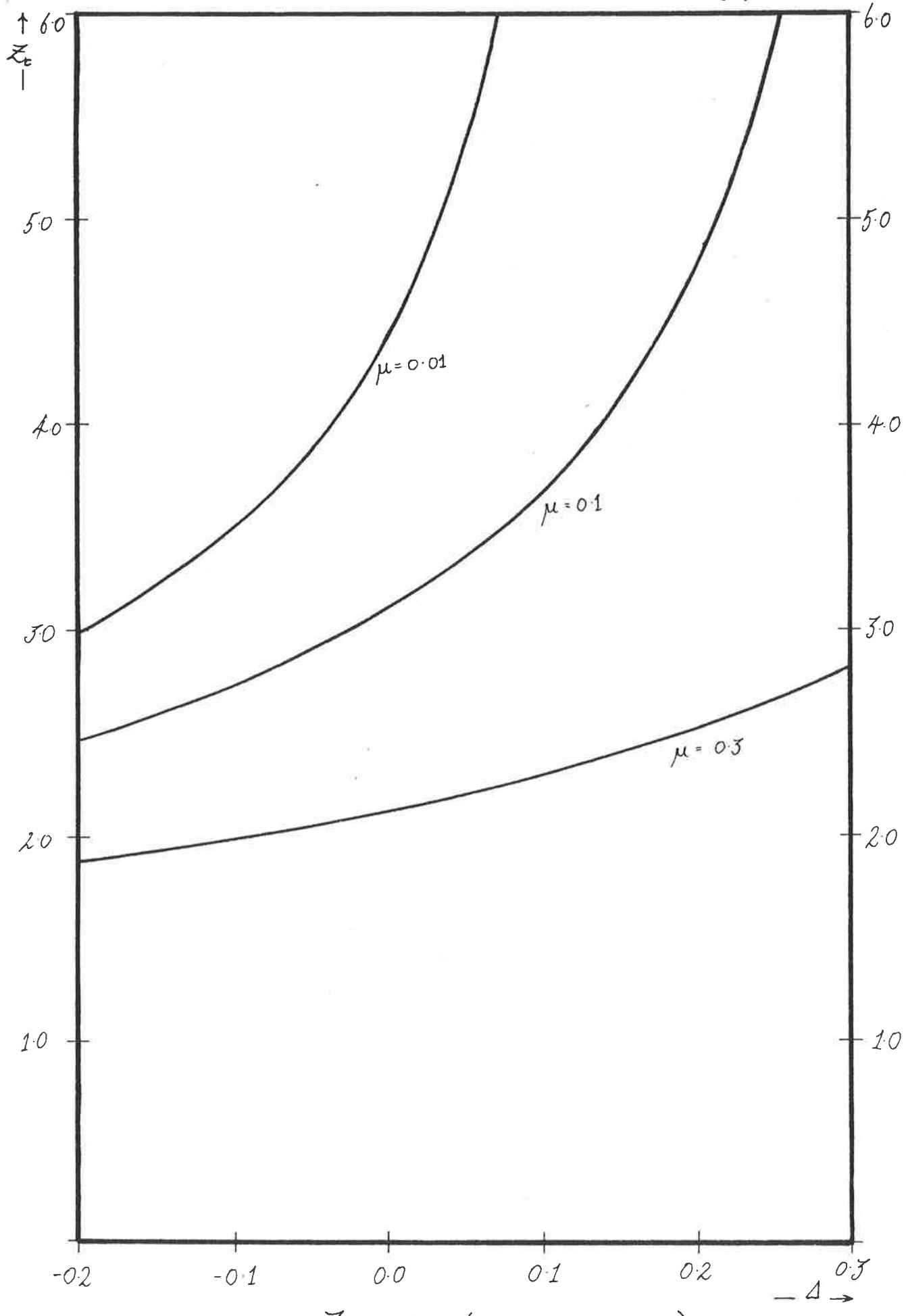

Z_c vs. Δ. ($\beta = 2.0$, $\sigma = 0.0$)

FIGURE 5.

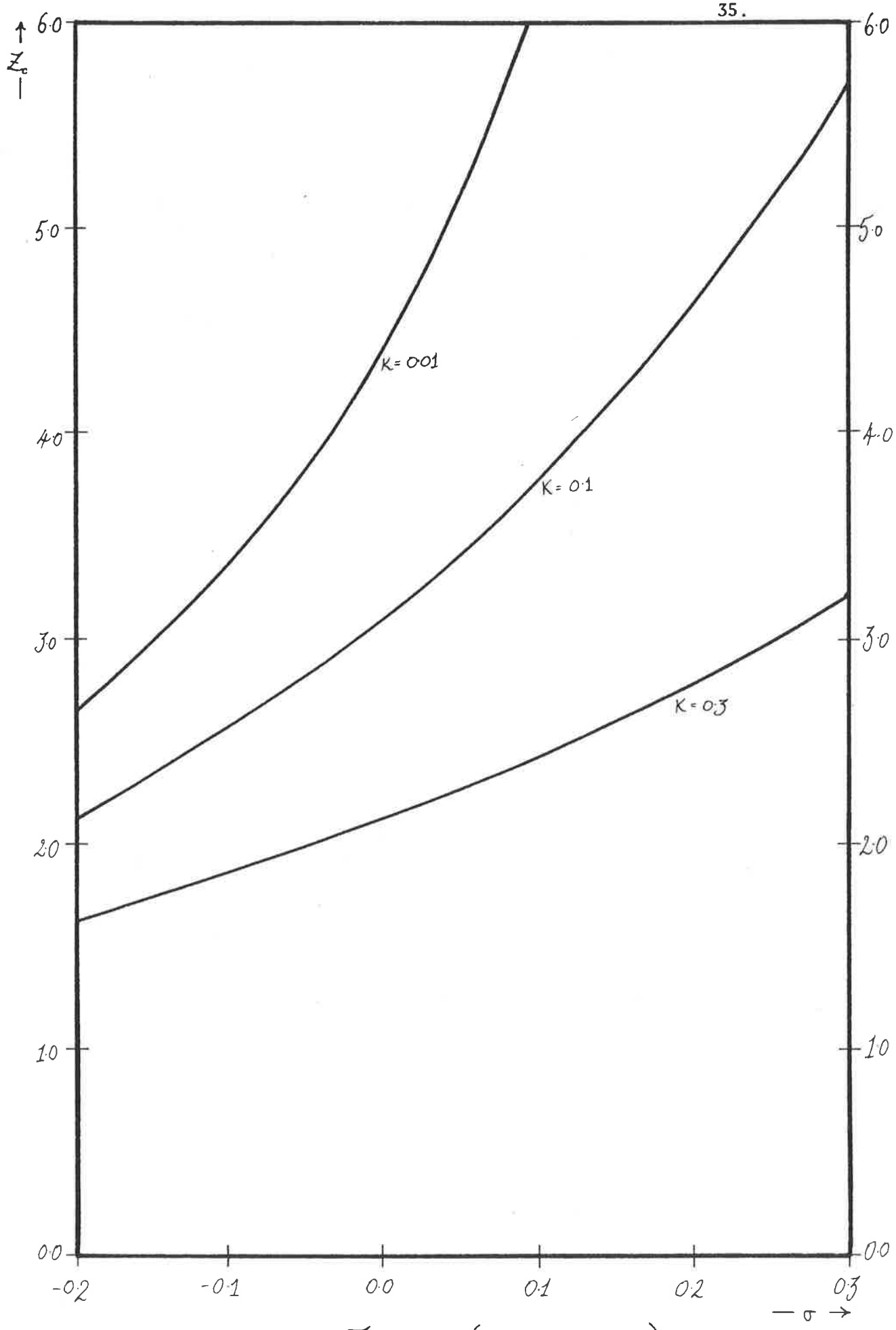

Z_c vs. σ. ($\Delta = 0{\cdot}0, \beta = 2{\cdot}0$)

FIGURE 6.

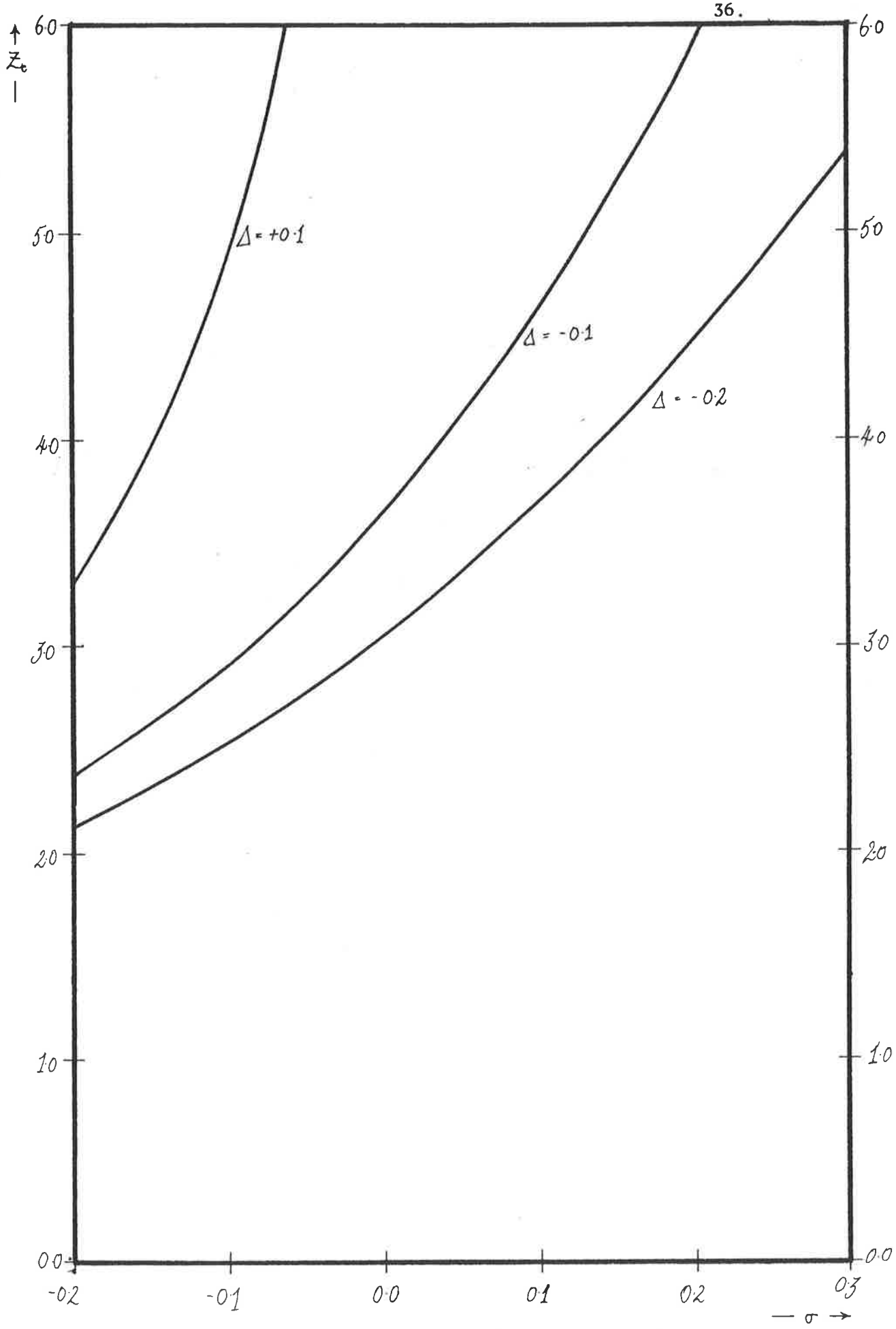

Z_c VS. σ. (κ=0·0, β=2·0)

FIGURE 7.

We have seen that thin jets are greatly influenced by surface tension and pressure forces. For this reason non-slender theory has been developed in the literature for the treatment of thin annular jets. References to this theory were given in the introduction. This theory is not entirely satisfactory and a consistent, formally correct theory will be given in a later section. For the moment however, we shall consider thin-slender-annular jets, via the equations already derived for thick jets, namely (3.5) - (3.7).

5. THIN-SLENDER ANNULAR JETS

The limit we are concerned with is

$$\beta \to 1 \quad , \tag{5.1}$$

and

$$b(z) \to a(z) \quad . \tag{5.2}$$

We shall put $h(z) = b(z) - a(z)$, that is, h is the thickness of the annular jet. We assume that equations (3.5) - (3.7) govern the jet behaviour, and we examine the limits (5.1) and (5.2) in these equations. The velocity $U(z)$, as given by (3.5), is unchanged. Equation (3.6), however, gives

$$U(z)a(z)h(z) = (\beta-1) \quad . \tag{5.3}$$

It is important to note that although we consider the formal limit $\beta \to 1$, we must retain the first order terms in $(\beta-1)$, as in (5.3). We also need expansions for $b'(z)^2-a'(z)^2$ and $\log (b/a)$. These are given by

$$b'(z)^2-a'(z)^2 = 2a'(z)[h'(z)] + O\{h^2\} \quad , \tag{5.4}$$

and

$$\log\left(\frac{b}{a}\right) = \frac{h}{a} + O\{h^2\} \ . \qquad (5.5)$$

We also reduce the term $\lambda''(z)$ to the equivalent in terms of $a(z)$ and $U(z)$. From (3.2) we find that

$$\lambda''(z) = \tfrac{1}{2}U''a^2 + 2U'aa' + Ua'^2 + Uaa'' \ . \qquad (5.6)$$

Using (5.3) to (5.6) in equation (3.7) results finally with

$$(1+2z)^{\frac{1}{4}}a''(z) + (1+2z)^{-\frac{1}{4}}a'(z) = -\frac{\kappa}{\beta-1} + \frac{\Delta}{\beta-1}a(z) \ , \qquad (5.7)$$

which is the fundamental equation for determining the shape of the annular jet, $a(z)$. It is immediately obvious that thin jets, $\beta \approx 1$, are indeed sensitive to κ and Δ. This follows from the "amplification" factor, $\frac{1}{(\beta-1)}$, multiplying the right-hand-side of (5.7). For a consistent theory we must have κ and Δ both of the order of $(\beta-1)$, which says that thin-slender-jets *do not exist* for large κ or Δ. Later, we shall see that this assumption is also inherent in the other thin annular jet, or "water-bell", theories. It is convenient to transform the equation (5.7) by putting

$$z = \tfrac{1}{2}\tau^2 + \tau \ . \qquad (5.8)$$

This leads to

$$\ddot{a}(\tau) = -\kappa'(\tau+1) + \Delta'(\tau+1)a(\tau), \qquad (5.9)$$

where $\kappa' = \frac{\kappa}{\beta-1}$ and $\Delta' = \frac{\Delta}{\beta-1}$. The dot denotes differentiation with respect to τ. The variable τ is *time-like*, and, as in Hoffman, Takahashi and Monson (1980), this problem may be tackled in an unsteady context where $\tau=0$ corresponds to the genesis of

the jet. Equation (5.9), with $\Delta'=0$, is obtained by the above authors, although their approach is inconsistent. The assumption of slenderness is made initially, however for most of the analysis the longitudinal curvature is retained. This is evident in the numerical work of Hoffman et al., since solutions of (5.9) with $\Delta'=0$ are compared with solutions from the fully non-linear equations, including longitudinal curvature, and are found to differ by no more than 5% for the appropriate range of the κ' parameter. We conclude then, that (5.9) is the correct, consistent, form for a slender, but thin annular jet. It appears that no solutions of (5.9) have been published for the case $\Delta' \neq 0$. Although these are straight forward to obtain they provide much insight into the dynamics of thin annular jets.

6. SOLUTIONS FOR THIN-SLENDER ANNULAR JETS

It is appropriate firstly to consider the gravity-free case, namely when $g \equiv 0$. The equation governing the bell's shape is

$$\ddot{a}(\tau) = -\kappa'' + \Delta'' a(\tau) \ , \tag{6.1}$$

where the constants κ'' and Δ'' are given by

$$\kappa'' = \frac{2T}{U_0^2 \rho a_0 (\beta-1)} \ , \tag{6.2}$$

and

$$\Delta'' = \frac{P}{\rho U_0^2 (\beta-1)} \ . \tag{6.3}$$

The solution of (6.1) subject to $a(0) = 1$, and $a'(0) = \sigma' = a_0'$ is

$$a(\tau) = -\frac{1}{2}\kappa''\tau^2 + \mathrm{Cosh}(\sqrt{\Delta''}\tau) + \frac{\sigma'}{\sqrt{\Delta''}}\mathrm{Sinh}(\sqrt{\Delta''}\tau) \ , \qquad (6.4)$$

provided $\Delta'' > 0$. In this case there is an under-pressure outside of the jet and collapse only occurs if

$$\mathrm{Cosh}(\sqrt{\Delta''}\tau_c) + \frac{\sigma'}{\sqrt{\Delta''}}\mathrm{Sinh}(\sqrt{\Delta''}\tau_c) = \frac{1}{2}\kappa''\tau_c^2 \ , \qquad (6.5)$$

has a real positive root, τ_c, for the collapse time τ_c. The collapse length Z_c, is given by

$$Z_c = \frac{1}{2}\tau_c^2 + \tau_c \ ,$$

from equation (5.8). In general (6.5) will only possess a root for τ_c if σ' is sufficiently large, in the negative sense. This can be seen if we consider $\kappa''=0$, that is neglect surface tension. τ_c is now a root of

$$\tanh(\sqrt{\Delta''}\tau_c) = -\frac{\sqrt{\Delta''}}{\sigma'} \ , \qquad (\sigma' \neq 0) \qquad (6.6)$$

an equation which has positive real roots only if

$$-1 < \frac{\sqrt{\Delta''}}{\sigma'} < 0 \ ,$$

whence $\sigma' < -\sqrt{\Delta''}$; that is, σ' is sufficiently small. In the case $\sigma' = 0$, there is no collapse.

We now suppose Δ'' is negative, say $\Delta'' = -\eta^2$. The solution of (6.1) in this case is

$$a(\tau) = -\frac{1}{2}\kappa''\tau^2 + \mathrm{Cos}(\eta\tau) + \frac{\sigma'}{\eta}\mathrm{Sin}(\eta\tau) \ . \qquad (6.7)$$

This results in the following equation for the collapse time τ_c,

$$\mathrm{Cos}(\eta\tau_c) + \frac{\sigma'}{\eta}\mathrm{Sin}(\eta\tau_c) = \frac{1}{2}\kappa''\tau_c^2 \ , \qquad (6.8)$$

which always has a positive real root for τ_c.

Thus we may conclude that bells with an overpressure, $\Delta'' < 0$, always collapse, regardless of the initial conditions. However for an underpressure, $\Delta'' > 0$, only jets initially directed *inward* at a sufficiently great angle (that is, those with σ' sufficiently negative) will collapse. This all applies of course to the gravity-free case. Never-the-less equation (5.9) may be solved, in general, in terms of Airy Functions (see Abramowitz and Stegun, Handbook of Mathematical Functions p. 446). These functions are however, qualitatively very similar to the hyperbolic cosine and sine functions when $\Delta' > 0$, and trigonometric functions when $\Delta' < 0$. It would seem then, that little new qualitative information is to be gained by repeating the above analysis with gravity included.

7. THIN ANNULAR SHEETS OF WATER

In the preceding sections we have described slender annular water jets. Proceeding from this, thin-slender jets were examined. It was found that such thin jets are extremely sensitive to surface tension forces, and to any pressure difference across the annulus. Indeed it was found that these pressures must be of $0\left\{\rho\frac{hu_0^2}{a_0}\right\}$ for the appropriate slender-flow approximations to be valid. In this section we analyze thin annular sheets of water, but with no *a priori* assumptions of slenderness. The analysis does however serve as a check on the previously obtained thin-slender jet equations, (5.7), since we may alternatively obtain these equations by assuming slenderness after thinness. The previous work published in connection with thin annular water sheets, for instance Boussinesq (1869) or

Lance and Perry (1953), have given solutions which appear to be for *arbitrary* values of the surface tension and pressure parameters, T and p. However, the thin-jet theory is really valid only for a restricted range of these parameters, and in the following consistent asymptotic analysis, we shall find necessary conditions on these parameters for the solutions, as given by the above authors, to be correct. (In the sense of asymptotic expansions).

We choose to analyze the problem from the exact (inviscid, irrotational) equations, under the sole premise that the annulus is thin. Consider the jet in the cylindrical polar coordinate system, as in the previous sections. Let $\phi(r,z)$ be the total, axisymmetric, velocity potential in the jet. We require that ϕ satisfies, as before, the axisymmetric Laplace equation,

$$\phi_{rr} + \frac{1}{r}\phi_r + \phi_{zz} = 0 \ . \tag{7.1}$$

Introducing the following notation for the free surfaces, namely that $r = f_+(z)$ represents the outer circular surface, while $r = f_-(z)$ represents the inner, we have the following two kinematic boundary conditions,

$$\phi_r = f_+'(z)\phi_z \quad \text{on} \quad r = f_+(z) \ , \tag{7.2}$$

and

$$\phi_r = f_-'(z)\phi_z \quad \text{on} \quad r = f_-(z) \ . \tag{7.3}$$

Physically (7.2) and (7.3) enforce the condition of no normal flow across the free boundaries f_+ and f_-. The exact dynamical equations (Constant pressure on the water air interface) on the surfaces $r = f_\pm(z)$ are given by

$$\tfrac{1}{2}\phi_r^2 + \tfrac{1}{2}\phi_z^2 + \frac{T}{\rho}\left\{\frac{\cos\psi_-}{f_-} + \frac{f_-''}{(1+f_-'^2)^{3/2}}\right\} + \frac{p}{\rho} = A \quad \text{on} \quad r = f_-(z), \tag{7.4}$$

and

$$\tfrac{1}{2}\phi_r^2 + \tfrac{1}{2}\phi_z^2 - \frac{T}{\rho}\left\{\frac{\cos\psi_+}{f_+} + \frac{f_+''}{(1+f_+'^2)^{3/2}}\right\} = A \quad \text{on} \quad r = f_+(z). \tag{7.5}$$

The derivation of these equations (in particular, the surface tension pressure terms) follow from §2, remembering that the curvature in the longitudinal plane on a surface $r = S(z)$ is given by $\dfrac{S''}{(1+S'^2)^{3/2}}$. ψ_-,ψ_+ are the angles that the surfaces $r = f_-(z), f_+(z)$ make with the horizontal, and so $\dfrac{\cos\psi_\pm}{f_\pm}$ is the radius of curvature, normal to the surface, in the azimuthal direction. Figure 8 illustrates this notation. The constant A, occurring in equation (7.4), (7.5) will be given a value later in this section. We now examine the limit $f_+ \to f_-$ in this system of equations (7.1) - (7.5).

8. EQUATIONS FOR A THIN JET

Firstly we put $a(z)$ equal to the mean surface shape, namely

$$a(z) = \frac{f_+(z)+f_-(z)}{2}, \tag{8.1}$$

and also put $h(z)$ equal to the half thickness of the annulus at the cross section z, so

$$h(z) = \frac{f_+(z)-f_-(z)}{2}. \tag{8.2}$$

The mathematical procedure to derive the equations for thin jets is to find a small h expansion of the relevant quantities of interest, and the exact equations which describe these quantities. As we shall see we need to retain first order terms in h, that is $O\{h\}$ terms, for a consistent theory. Alternatively this may be thought of as neglecting error terms of $O\{h^2\}$.

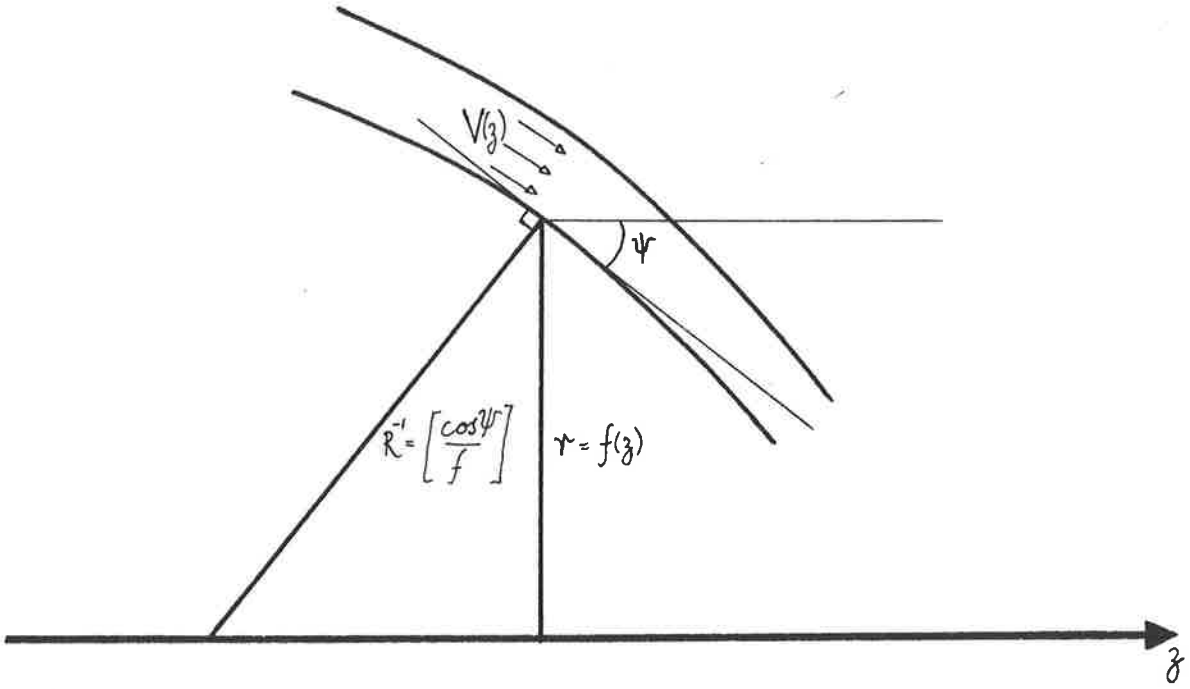

Radius of Curvature (R) (azimuthal plane)

FIGURE 8.

We now formulate the problem in a new coordinate system, (ρ,θ,ξ), defined as

$$\xi = z, \tag{8.3}$$

and

$$\rho = r - a(z), \tag{8.4}$$

from the (r,θ,z) coordinate system. The axial angle coordinate θ is actually redundant, since the jet is supposed to be axisymmetric. The (ρ,θ,ξ) coordinate system is not orthogonal and we can expect considerable change to the equations describing the jet. The differential operators in equations (7.1) - (7.5) are now given in the new coordinate system by replacing $\frac{\partial}{\partial z}$ with $\frac{\partial}{\partial \xi} - a'\frac{\partial}{\partial \rho}$ and $\frac{\partial}{\partial r}$ by $\frac{\partial}{\partial \rho}$. The axisymmetric Laplace equation, (7.1), becomes

$$(1+a'^2)\phi_{\rho\rho} + \frac{1}{a+\rho}\phi_\rho + \phi_{\xi\xi} - 2a'\phi_{\xi\rho} - a''\phi_\rho = 0 , \tag{8.5}$$

following the above substitutions. Furthermore the kinematic boundary conditions, (7.2) and (7.3) become,

$$\phi_\rho = (a'+h')[\phi_\xi - a'\phi_\rho] \quad \text{on} \quad \rho = h \tag{8.6}$$

and

$$\phi_\rho = (a'-h')[\phi_\xi - a'\phi_\rho] \quad \text{on} \quad \rho = -h . \tag{8.7}$$

The dynamic conditions will not be needed at the moment, and the appropriate transformed equations are given later. In the (ρ,θ,ξ) coordinate system we have the jet region defined by

$$-h \leqslant \rho \leqslant h, \quad \text{for} \quad \xi \geqslant 0 . \tag{8.8}$$

Thus the thin-annular jet potential, ϕ, should be given by a small ρ expansion, since for a thin annulus $h \ll 1$. This suggests trying a velocity potential of the form,

$$\phi(\rho,\xi) = \Phi_0(\xi) + \rho\Phi_1(\xi) + \frac{1}{2}\rho^2\Phi_2(\xi) + \ldots \quad , \tag{8.9}$$

where $\Phi_0,\Phi_1,\Phi_2,\ldots$ are yet to be determined functions of ξ. In practice we truncate the expansion in (8.9) after the three terms shown. Using further terms leads to a solution of higher order accuracy but the resulting system of equations becomes exceedingly difficult to solve. The zero order terms in h (i.e. $0\{h^0\}$) from equation (8.5) give

$$(1+a'^2)\Phi_2 + \frac{1}{a}\Phi_1 + \Phi_0'' - 2a'\Phi_1' - a'\Phi_1 = 0 \ . \tag{8.10}$$

In obtaining equation (8.10) we have neglected terms of $0\{\rho\}$. Similarly the boundary conditions (8.6) and (8.7) become,

$$\Phi_1 + h\Phi_2 = (a'+h')[\Phi_0'+h\Phi_1-a'\Phi_1-a'h\Phi_2], \tag{8.11}$$

and

$$\Phi_1 - h\Phi_2 = (a'-h')[\Phi_0'-h\Phi_1-a'\Phi_1+a'h\Phi_2], \tag{8.12}$$

where zero-order and first-order terms in h and h' have been retained. Intuitively we justify retaining these terms as follows. The leading-order terms in equations (8.5), (8.6) and (8.7) convey information only concerning the *mean* shape $a(z)$. The first-order terms of (8.6) and (8.7), however, describe the *thickness* effects, which must be treated as an unknown, and so retained. The equations (8.10), (8.11) and (8.12) together with two dynamical equations (zero and first order equations) gives five ordinary differential equations for the five unknown functions Φ_0,Φ_1,Φ_2,a and h. In principle this can be solved.

Adding (8.11) and (8.12) and neglecting $0\{h\}$ and $0\{h'\}$ terms, results in

$$a'\Phi_0' = (1+a'^2)\Phi_1 \ , \tag{8.13}$$

while subtracting (8.12) from (8.11) gives

$$(1+a'^2)\Phi_2 = a'\Phi_1' + \Phi_0'\frac{h'}{h} - a'\Phi_1\frac{h'}{h} \ . \tag{8.14}$$

Equation (8.13) is the zero-order kinematic condition and equation (8.14) the first order condition. While physical significance can be attached to these equations there is little benefit from doing this at this stage. From this set of equations (8.10), (8.13) and (8.14) we can expect to derive a conservation law, analogous to equation (3.3), expressing conservation of mass along the jet. Differentiation of (8.13), with respect to ξ, results in

$$\Phi_0'' = (a' + \frac{1}{a'})\Phi_1' + (a'' - \frac{a''}{a'^2})\Phi_1 \ , \tag{8.15}$$

and upon elimination of Φ_0'', Φ_2 between equations (8.15), (8.10) and (8.14) leads to

$$\Phi_1[h + \frac{ah'}{a'} - \frac{a''ah}{a'^2}] + \frac{ah}{a'}\Phi_1' = 0 \tag{8.16}$$

which simply states

$$\frac{d}{d\xi}[\frac{ah}{a'}\Phi_1] = 0 \ , \tag{8.17}$$

or upon integration with respect to ξ,

$$\Phi_1\frac{ah}{a'} = \text{Constant}, \quad C_0 \text{ say.} \tag{8.18}$$

By virtue of equation (8.13) we then have

$$\frac{ah\Phi_0'}{(1+a'^2)} = C_0 \ , \tag{8.19}$$

which is the appropriate conservation of mass constraint. To see

this more clearly we consider $V(\xi)$, the velocity of the water tangential to the sheet. Locally, at the section z, the sheet has mean slope $a'(z)$ and so makes an angle ψ with the horizontal such that $\tan\psi = a'$. Thus from simple trigonometric rules we have

$$\cos\psi = (1+a'^2)^{-\frac{1}{2}} \quad \text{and} \quad \sin\psi = a'(1+a'^2)^{-\frac{1}{2}}.$$

The tangential velocity, $V(\xi)$, is then given by, to zeroth-order,

$$V(\xi) = \cos\psi\,\phi_z + \sin\psi\,\phi_r \ , \tag{8.20}$$

which reduces to

$$V(\xi) = \frac{\Phi_0'}{(1+a'^2)^{\frac{1}{2}}} \ , \tag{8.21}$$

in terms of our "thin-jet functions". Equation (8.19) now has the form

$$a(\xi)V(\xi)h(\xi)\cos\psi = C_0 \ , \tag{8.22}$$

which represents constant mass flux in the jet since $h(\xi)\cos\psi$ is the *normal* thickness of the annulus at each ξ cross section. This equation is of course intuitively obvious and has been obtained by previous investigators. It now remains to consider the appropriate form of the dynamic equations. From these equations we can expect to derive the velocity $V(\xi)$, as a function of ξ alone, and an equation representing a balance of inertia normal to the stream. Some preliminary expansions will be needed, these are

$$\frac{\cos\psi_{\pm}}{f_{\pm}} = \frac{\cos\psi}{a}\{1 + O\{h\}\} \ , \tag{8.23}$$

and

$$\frac{1}{(1+f'^2)^{3/2}} = \frac{1}{(1+a'^2)^{3/2}}\{1 + O\{h'\}\} . \qquad (8.24)$$

Equations (8.23) and (8.24) give the zeroth-order curvature terms, and it will be seen that terms of this order only shall be needed in the following analysis.

9. THE DYNAMIC EQUATIONS

The exact form of these equations, (7.4) and (7.5) when transformed into the (ρ,θ,ξ) coordinate system becomes

$$\frac{1}{2}\phi_\rho^2 + \frac{1}{2}(\phi_\xi - a'\phi_\rho)^2 - g\xi + \frac{T}{\rho}\left\{\frac{\cos\psi_-}{f_-} + \frac{f_-''}{(1+f'^2)^{3/2}}\right\} + \frac{p}{\rho} = A \quad \text{on} \quad \rho=-h, \qquad (9.1)$$

and

$$\frac{1}{2}\phi_\rho^2 + \frac{1}{2}(\phi_\xi - a'\phi_\rho)^2 - g\xi - \frac{T}{\rho}\left\{\frac{\cos\psi_+}{f_+} + \frac{f_+''}{(1+f_+'^2)^{3/2}}\right\} = A \quad \text{on} \quad \rho=h. \qquad (9.2)$$

Substitution of the expansion given in equation (8.9), and the zeroth order curvature terms, leads to the following set of equations,

$$\frac{1}{2}[\Phi_1+h\Phi_2]^2+\frac{1}{2}[\Phi_0'+h\Phi_1-a'\Phi_1-a'h\Phi_2]^2-g\xi+\frac{T}{\rho}\left\{\frac{\cos\psi}{a} + \frac{a''}{(1+a'^2)^{3/2}}\right\} + \frac{p}{\rho} = A, \qquad (9.3)$$

and

$$\frac{1}{2}[\Phi_1-h\Phi_2]^2+\frac{1}{2}[\Phi_0'-h\Phi_1-a'\Phi_1+a'h\Phi_2]^2-g\xi-\frac{T}{\rho}\left\{\frac{\cos\psi}{a} + \frac{a''}{(1+a'^2)^{3/2}}\right\} = A. \qquad (9.4)$$

Immediately we see that $\frac{p}{\rho}$ and $\frac{T}{\rho}\left\{\frac{\cos\psi}{a} + \frac{a''}{(1+a'^2)^{3/2}}\right\}$ must be no more than $O\left\{\frac{hU_0^2}{a}\right\}$, where U_0 is a measure of longitudinal jet velocity. This is because the above terms are independent of h, yet cannot satisfy both of equation (9.3) and (9.4) to *zeroth* order. There is no avoiding this constraint for $\frac{p}{\rho}$; thus if $\frac{p}{\rho} \gg \frac{hU_0^2}{a}$ equations (9.3), (9.4) cannot both be satisfied in a small h limit. This merely states that thin annular jets cannot sustain a large pressure

difference across the annulus. In practice if there is a large pressure difference, the water bell either collapses or expands extremely rapidly, and an alternative formulation, rather than the one we have chosen, is necessary to describe this behaviour.

For the surface-tension pressure there are two possibilities whereby the constraint may be satisfied. Firstly, the numerical value of $\frac{T}{\rho}$ may be sufficiently small so that $\frac{T}{\rho}\left\{\frac{\cos\psi}{a} + \frac{a''}{(1+a'^2)^{3/2}}\right\}$ is of $O\left\{\frac{hU_0^2}{a}\right\}$, and in general this will be so. However, if h is exceedingly small, and the mass flux not too great, then it is necessary that the zeroth-order term $\frac{\cos\psi}{a} + \frac{a''}{(1+a'^2)^{3/2}}$ be small, that is the formally correct equation (in the sense of asymptotic expansions) for the water bell's radius $a(\xi)$ is

$$\frac{1}{a} + \frac{a''}{(1+a'^2)} = 0 \ , \qquad (9.5)$$

since $\cos\psi = (1+a'^2)^{-\frac{1}{2}}$. This states, to leading order, that the water bell is a spherical shell, or bubble, given by

$$a(z) = (1+\sigma^2) - (z-\sigma)^2 \ , \qquad (9.6)$$

where σ is the mean slope of the sheet at $z=0$. This result is to be expected whenever, as here, surface tension is the dominant force. It simply says the water bell is a "bubble" to leading order.

For the remainder of this section we assume that the former condition holds, that is, that $\frac{T}{\rho}$ is small[1]. The leading order

---

[1] In C.G.S. system $\frac{T}{\rho a} \sim 72\ \mathrm{cm^2 s^{-2}}$, and for $a = 1$ cm, $U_0 = 100\ \mathrm{cm\ s^{-1}}$ we have

$$h \sim \frac{1}{10}\ \mathrm{cm} \Rightarrow \frac{hU_0^2}{a_0} \sim 10^3\ \mathrm{cm^2 s^{-2}}$$

$$h \sim \frac{1}{100}\ \mathrm{cm} \Rightarrow \frac{hU_0^2}{a_0} \sim 10^2\ \mathrm{cm^2 s^{-2}}$$

equation from (9.3) and (9.4) is obtained by adding these two equations, and neglecting $O\{h\}$ terms. We find that

$$\frac{1}{2}(\Phi_0'^2 - (1+a'^2)\Phi_1^2) - g\xi = A \ , \tag{9.6}$$

which from equation (8.13) gives

$$\frac{\Phi_0'^2}{(1+a'^2)} = U_0^2 + 2g\xi$$

or

$$V(\xi) = (U_0^2 + 2g\xi)^{\frac{1}{2}} \ , \tag{9.7}$$

where we suppose the "initial" velocity $V(0)$ is U_0, thus determining the constant A. This too is a familiar result, being obtained by previous authors. It reflects the fact that the normally directed pressure and surface tension forces do not accelerate the fluid tangentially along the jet; such acceleration is solely accomplished by gravity.

Subtracting (9.4) from (9.3) leads to the first order equation,

$$h(\Phi_1\Phi_2+\Phi_0'\Phi_1'-a'\Phi_0'\Phi_2-a'\Phi_1\Phi_1'+a'^2\Phi_1\Phi_2)+\frac{T}{\rho}\left(\frac{1}{a(1+a'^2)^{\frac{1}{2}}} + \frac{a''}{(1+a'^2)^{3/2}}\right)+\frac{p}{\rho} = 0. \tag{9.8}$$

However this can be rearranged to yield,

$$\frac{h\Phi_1\Phi_1'}{a'} + \frac{T}{\rho}\left\{\frac{1}{a(1+a'^2)^{\frac{1}{2}}} + \frac{a''}{(1+a'^2)^{3/2}}\right\} + \frac{p}{\rho} = 0 \ , \tag{9.9}$$

where we have used equation (8.13). Now $\frac{h\Phi_1}{a'}$ can be replaced by C_0/a, from equation (8.18), and since, from (8.13)

$$\Phi_1 = \frac{a'}{(1+a'^2)^{\frac{1}{2}}} V(\xi) \ , \text{ we have}$$

$$\Phi_1' = \frac{a'}{(1+a'^2)^{1/2}} V(\xi) + \frac{a''}{(1+a'^2)^{3/2}} V(\xi) \quad . \qquad (9.10)$$

The resulting form of the first-order equation after substituting (9.10) in (9.9) is

$$\frac{C_0 a''(U_0^2+2g\xi)}{a(1+a'^2)^{3/2}} + \frac{C_0\, g\, a'}{a(1+a'^2)^{1/2}(U_0^2+2g\xi)^{1/2}} + \frac{T}{\rho}\left\{\frac{1}{a(1+a'^2)^{1/2}} + \frac{a''}{(1+a'^2)^{3/2}}\right\} + \frac{p}{\rho} = 0. \quad (9.11)$$

A more convenient form is obtained when *all* lengths are scaled with respect to $\frac{U_0^2}{g}$, which gives

$$\frac{a''}{a(1+a'^2)^{3/2}}(1+2\xi)^{1/2} + \frac{(1+2\xi)^{-1/2} a'}{a(1+a'^2)^{1/2}} + \alpha\left\{\frac{1}{a(1+a'^2)^{1/2}} + \frac{a''}{(1+a'^2)^{3/2}}\right\} + \beta = 0, \quad (9.12)$$

where the parameters α, β are given by

$$\alpha = \frac{T}{\rho g a_0 h_0 \cos\psi_0} \quad ,$$

and

$$\beta = \frac{p U_0^2}{\rho g^2 a_0 h_0 \cos\psi_0} \quad . \qquad (9.13)$$

a_0 and h_0 are the "initial" (z=0) mean radii and half thickness respectively, while ψ_0 is the initial angle of projection. Equation (9.12) represents a balance of inertia normal to the water sheet. Direct derivation of equation (9.12) is possible from physical arguments, based on the "balance of inertia" concept. This is precisely the equation obtained by Lance and Perry (1953), and subsequently solved by them, for a variety of values of the α and β parameters.

We choose to check the slender jet equation (5.7) from equation (9.12). For the jet to be slender requires that a' is everywhere

small; thus we elect to neglect this quantity squared, and additionally we neglect the longitudinal curvature since $\frac{a''}{(1+a'^2)^{3/2}} \ll \frac{1}{a(1+a'^2)^{1/2}}$. Thus (9.12) reduces to

$$(1+2\xi)^{1/2}a'' + \frac{a'}{(1+2\xi)^{1/2}} = -\alpha' + \beta' a \ , \qquad (9.14)$$

with the new constants $\alpha' = \frac{T}{\rho g a_0 h_0}$ and $\beta' = -\frac{pU_0^2}{\rho g^2 a_0 h_0}$. This is exactly equation (5.7) with $\alpha' = \kappa'$ and $\beta' = \Delta'$, obtained in §5 from the thick-slender jet equations, and verifies the thin-slender jet results thus far obtained. That is, it is of no consequence in which order we carry out the limits of slenderness and thinness.

10. CONCLUSIONS

We do not solve the ordinary differential equation (9.12) for the radius of water-bells, as this has been extensively covered by previous authors. In general the solutions must be computed numerically, although when $g\equiv 0$ and $\beta=0$ Taylor (1959) has obtained exact analytic solutions. What is interesting from these solutions is the formation of cusps on the sheet at finite radii, that is before collapse. This phenomenon is entirely absent from the slender jet theories and one may expect that the effects of thickness, in an exact theory, counteract this.

The formal asymptotic derivation of equation (9.12) has shown several new points, which were somewhat obscured by the previous derivations. Most importantly the pressure jump parameter $\frac{p}{\rho}$ is necessarily small, otherwise a cross flow within the annulus, of

comparable order to the tangential flow, is needed to satisfy the dynamic boundary conditions. This would then require a full solution of the exact equations, which at present is not considered. We have also seen that if the sheet is too thin and the mass flux (that is velocity U_0) small the water bell assumes the shape of a sphere, as if it were a static bubble. This of course is only valid away from the collapse point, where in general our solutions are invalid.

CHAPTER 3

STABILITY OF ANNULAR COLUMNS OF WATER

1. INTRODUCTION

When a jet, such as those described in the previous chapters, issues into the ambient atmosphere it will be subject to a number of disturbances, not considered thus far in this thesis. These disturbances, perhaps vibrations or imperfections of the nozzle, or possibly small variations in the atmospheric pressure along the jet, may ultimately be responsible for breakup of the jet. In effect, this means that the disturbance grows in time (temporally) or in space, say along the jet (spatially).

This phenomenon, known as instability, has been widely investigated for round jets, as far back as Rayleigh (1879). Subsequent authors have extended and improved on Rayleigh's analysis, to the point where non-linear aspects of jet fragmentation can be described.

The case for annular jets is much less advanced. The analysis for linear, temporal instability has been provided by Ponstein (1959), but, as we shall see, some of his conclusions are erroneous, and a more detailed examination of these results is warranted. We also discuss some aspects of spatial instability, as it seems that this type of instability is more plausible in practical situations (see Keller, Rubinov and Tu (1973)).

2. TEMPORAL INSTABILITY OF AN ANNULAR COLUMN

To illustrate the mechanism for jet breakup we examine an annular cylindrical jet, moving with constant velocity U_0. We

neglect gravity; thus, the unperturbed jet always has $r = a_0$ and $r = b_0$ for its inner and outer free surfaces, respectively. We assume that the jet extends from $z = -\infty$ to $z = \infty$; that is, there is no nozzle in the region of flow. If there is a nozzle, temporal instability is no longer satisfactory physically. At some time, $t=0$ say, the surfaces of the jet are perturbed. The exact nature of this disturbance is unnecessary to know, since, as the following analysis is linear, it is appropriate to consider Fourier components of such perturbations.

Let $\phi(r,z,t)$ be the velocity potential in the jet and $r = \eta_{1,2}(z)$ the inner and outer surfaces respectively, after $t=0$. We assume that the disturbances to the free surfaces are small, and take the following form,

$$\eta_1(z) = a_0 + \varepsilon_1 e^{\sigma t} e^{ikz} , \qquad (2.1)$$

and

$$\eta_2(z) = b_0 + \varepsilon_2 e^{\sigma t} e^{ikz} . \qquad (2.2)$$

σ is the principal unknown, since σ real and $\sigma > 0$ gives the rate at which the disturbance grows in time.

We note that (2.1) and (2.2) only admit axisymmetric modes of disturbances; however, as shown by Ponstein (1959), these are the most important, as far as instability is concerned. k is essentially a *real* input parameter; thus, our task is to find a dispersion relationship $\sigma = \sigma(k)$. The concept introduced by Rayleigh, that of mode of maximum instability, now says that the jet breaks up due to disturbances with $k = k_{max}$, where $\sigma(k_{max})$ is the largest positive, real value of $\sigma(k)$.

3. EQUATIONS OF MOTION

We assume that the jet is inviscid, and is flowing irrotationally. Thus we require ϕ, the velocity potential, to satisfy the axisymmetric Laplace equation

$$\phi_{rr} + \frac{1}{r}\phi_r + \phi_{zz} = 0, \tag{3.1}$$

in cylindrical polar coordinates. Furthermore, we try for a solution of the form,

$$\phi(r,z,t) = e^{\sigma t} e^{ikz} \Phi(r), \tag{3.2}$$

which, from (3.1), immediately gives

$$\Phi(r) = AI_0(kr) + BK_0(kr) , \tag{3.3}$$

where I_0 and K_0 are modified Bessel functions of zeroth order. A and B are yet to be determined constants.

Before introducing the boundary conditions for this problem, it is appropriate to transform the spatial coordinate slightly. This is accomplished by replacing z with $z^* - U_0 t$, which reduces the jet-like character to a static cylinder-like character. The boundary conditions are more convenient in this latter context, and for the remainder of this chapter we assume this substitution has been made, dropping however the * superscript. Moreover, because the disturbances on the column are small we shall approximate the boundary conditions to leading order in these disturbances.

4. KINEMATIC BOUNDARY CONDITIONS

The kinematic boundary conditions (no flow across the free boundaries) are approximated by

$$\frac{\partial \eta_{1,2}}{\partial t} = \phi_r \quad \text{on} \quad r = \eta_{1,2}(z), \tag{4.1}$$

where we have neglected $\eta'_{1,2}\phi_z$, which is $<<$ than $\frac{\partial \eta_{1,2}}{\partial t}$ or ϕ_r. Furthermore we evaluate (4.1) on $r = a_0, b_0$, to give the leading-order equations, which are,

$$\varepsilon_1 \omega = k\{AI_1(ka_0) - BK_1(ka_0)\}, \tag{4.2}$$

and

$$\varepsilon_2 \omega = k\{AI_1(kb_0) - BK_1(kb_0)\}. \tag{4.3}$$

In (4.2) and (4.3) ω is related to σ by

$$\omega = \sigma - kU_0 i, \tag{4.4}$$

because of the new, now "moving", coordinate system. I_1 and K_1 are modified Bessel functions of first order.

5. DYNAMIC BOUNDARY CONDITIONS

Before introducing the appropriate pressure conditions on the boundaries $r = \eta_{1,2}(z)$, we consider the undisturbed annular cylinder. Given that we know the free surfaces $r = a_0$ and $r = b_0$ this uniquely prescribes the pressure difference (cf. Chapter 2) to be

$$p = -T\left(\frac{1}{b_0} + \frac{1}{a_0}\right), \tag{5.1}$$

that is an underpressure which keeps the surface tension forces in equilibrium. If the pressure difference between the inside and outside of the annulus is not the value given in (5.1) then the straight annular cylinder is not an equilibrium situation, and in actual fact must be either "contracting" or "expanding" in the sense of Chapter 2. We cannot study the instability of these jets with the analytic techniques of this chapter. However, we can

expect some insight into the general mechanism of instability, for annular jets, by studying the annular cylinder subject to (5.1).

The appropriate approximation to the dynamic boundary condition is given by (Bernoulli's Equation)

$$\phi + \frac{p}{\rho} = \frac{p_e}{\rho} \quad \text{on} \quad r = a_0, b_0 \ . \tag{5.2}$$

Here, we have neglected the velocity head, which is small, and again evaluated the expression on $r = a_0, b_0$. $\frac{p}{\rho}$ is the pressure on the surface of the jet resulting from surface tension forces and pressure differences across the annulus. $\frac{p_e}{\rho}$ is the equilibrium pressure outside the jet, that is for $r > b_0$.

Equation (5.2), upon invoking (5.1) and using the surface-tension-curvature results from Chapter 2, leads to the following two equations,

$$\omega\{AI_0(ka_0) + BK_0(ka_0)\} + \varepsilon_1 \frac{T}{\rho}\{\frac{1}{a_0^2} - k^2\} = 0 \ , \tag{5.3}$$

and

$$\omega\{AI_0(kb_0) + BK_0(kb_0)\} - \varepsilon_2 \frac{T}{\rho}\{\frac{1}{b_0^2} - k^2\} = 0 \ . \tag{5.4}$$

These two equations, together with (4.2) and (4.3) give four equations for the unknowns, ω, A, B and

$$\gamma = \frac{\varepsilon_1}{\varepsilon_2} \ . \tag{5.5}$$

Thus in principal we can now find ω, A, B and γ as functions of k, and, in particular, determine the dispersion relationship $\omega = \omega(k)$.

6. THE DISPERSION RELATIONS

It is convenient to non-dimensionalize (4.2), (4.3), (5.3) and (5.4) by scaling radial and axial lengths with respect to b_0. The following equations result,

$$\gamma\epsilon_2\omega = \kappa\{AI_1(\kappa\beta) - BK_1(\kappa\beta)\} , \tag{6.1}$$

$$\epsilon_2\omega = \kappa\{AI_1(\kappa) - BK_1(\kappa)\} , \tag{6.2}$$

$$\omega\{AI_0(\kappa\beta) + BK_0(\kappa\beta)\} = -\gamma\epsilon_2\frac{T}{\rho b_0^3}\left\{\frac{1}{\beta^2} - \kappa^2\right\} , \tag{6.3}$$

and

$$\omega\{AI_0(\kappa) + BK_0(\kappa)\} = \epsilon_2\frac{T}{\rho b_0^3}\{1 - \kappa^2\} , \tag{6.4}$$

where $\kappa = kb_0$ and $\beta = a_0/b_0$. Thus, the jet we are now concerned with has outer radius 1.0 and has $0 < \beta < 1$. Eliminating the constants A and B from these four equations leads to

$$\frac{\omega^2}{\kappa\Delta}\{\gamma\{I_0(\kappa\beta)K_1(\kappa)+K_0(\kappa\beta)I_1(\kappa)\}-\{I_0(\kappa\beta)K_1(\kappa\beta)+K_0(\kappa\beta)I_1(\kappa\beta)\}\}$$

$$= -\gamma\frac{T}{\rho b_0^3}\left\{\frac{1}{\beta^2} - \kappa^2\right\} , \tag{6.5}$$

and

$$\frac{\omega^2}{\kappa\Delta}\{\gamma[I_0(\kappa)K_1(\kappa)+K_0(\kappa)I_1(\kappa)]-[I_0(\kappa)K_1(\kappa\beta)+K_0(\kappa)I_1(\kappa\beta)]\}$$

$$= \frac{T}{\rho b_0^3}\{1 - \kappa^2\} , \tag{6.6}$$

where $\Delta = K_1(\kappa)I_1(\kappa\beta) - I_1(\kappa)K_1(\kappa\beta) \neq 0$, for any real κ,β except if $\beta = 1$. In addition, if we scale time with respect to $\left(\frac{T}{\rho b_0^3}\right)^{1/2}$, and use the relations 9.6.15 from page 375 of Abramowitz and Stegun (1972) the following equations result, namely

$$\frac{\omega^2}{\kappa\Delta}\{\gamma[I_0(\kappa\beta)K_1(\kappa)+K_0(\kappa\beta)I_1(\kappa)] - \frac{1}{\kappa\beta}\} = -\gamma\left\{\frac{1}{\beta^2} - \kappa^2\right\} , \tag{6.7}$$

and

$$\frac{\omega^2}{\kappa\Delta}\{\frac{\gamma}{\kappa} - [I_0(\kappa)K_1(\kappa\beta)+K_0(\kappa)I_1(\kappa\beta)]\} = \{1 - \kappa^2\}. \tag{6.8}$$

Ponstein (1959) elects to eliminate γ from (6.7), (6.8) and obtain a fourth order polynomial for ω, in fact a quadratic in ω^2, where the coefficients are functions of κ. This can be misleading, and we shall see it is necessary to retain both γ and ω to clearly understand the instability process. This is particularly so when considering the $\beta \to 0$ limit, when Rayleigh's results should be obtained. The equations we choose to work with are the following,

$$\gamma^2\left[\frac{\frac{1}{\beta^2}-\kappa^2}{1-\kappa^2}\right]\frac{1}{\kappa}+\gamma\left[I_0(\kappa\beta)K_1(\kappa)+K_0(\kappa\beta)I_1(\kappa)-\left(\frac{\frac{1}{\beta^2}-\kappa^2}{1-\kappa^2}\right)(I_0(\kappa)K_1(\kappa\beta)+K_0(\kappa)I_1(\kappa\beta))\right]$$

$$-\frac{1}{\kappa\beta}=0\ , \qquad (6.9)$$

which arises when $\frac{\omega^2}{\kappa\Delta}$ is eliminated between (6.7) and (6.8), and

$$\omega^2=\frac{\kappa\Delta\ \{1-\kappa^2\}}{\frac{\gamma}{\kappa}-\left[I_0(\kappa)K_1(\kappa\beta)+K_0(\kappa)I_1(\kappa\beta)\right]}\ . \qquad (6.10)$$

(6.10) is a simple rearrangement of (6.8), however this emphasises our approach. Namely, for a particular κ, we solve (6.9) for two roots γ_1 and γ_2 which represent two different modes of instability. Corresponding to each of these modes, there is a growth rate, in time, given by substituting γ_1 and γ_2 into (6.10).

We may represent the solution of equation (6.9) as

$$\gamma_{i,2}=\frac{-g\pm\left(g^2+4\left(\frac{\frac{1}{\beta^2}-\kappa^2}{1-\kappa^2}\right)\frac{1}{\kappa^2\beta}\right)^{\frac{1}{2}}}{2\left(\frac{\frac{1}{\beta^2}-\kappa^2}{1-\kappa^2}\right)\frac{1}{\kappa}}\ , \qquad (6.11)$$

where g is the coefficient of γ in (6.9). Now the discriminant (terms under the square root sign in (6.11)) can be reduced to the

discriminant arising in the quadratic equation examined by Ponstein (1959), which can be shown to be non-negative. Thus equation (6.9) always has real roots γ_1, γ_2. The physical significance of this is that for $\gamma > 0$ the disturbance on the outer free surface has the same phase as the disturbance on the inner free surface. If $\gamma < 0$ the disturbance on the inner free surface lags the disturbance on the outer free surface by half a wavelength, spatially. (That is, considering the jet at any particular instant of time.)

The magnitude of γ indicates to what extent a disturbance is amplified from the inner surface to the outer surface or vice versa, and this provides important qualitative information on the breakup of annular columns.

Because γ is always real, equation (6.10) always gives ω^2 real, or $(\sigma - iU_0k)^2$ [scaled with respect to $\left(\frac{T}{\rho b_0^3}\right)^{1/2}$] real. Thus, as far as instability is concerned, that is for roots with σ real and positive, we only need consider positive values of ω^2 from equation (6.10). Figures 1 to 4 present the results for $\sigma(\kappa)$ and $\gamma(\kappa)$, for two different modes of instability. These modes have clear physical interpretations in the two limiting cases $\beta \to 0$ and $\beta \to 1$. However in the intermediate region their nature is somewhat more obscure.

7. RESULTS

The first important difference between the modes of instability, is the scales on the vertical axes. The axis for mode-one disturbances is stretched, approximately by a factor of 1000, relative to the axis for mode-two disturbances. It is not correct,

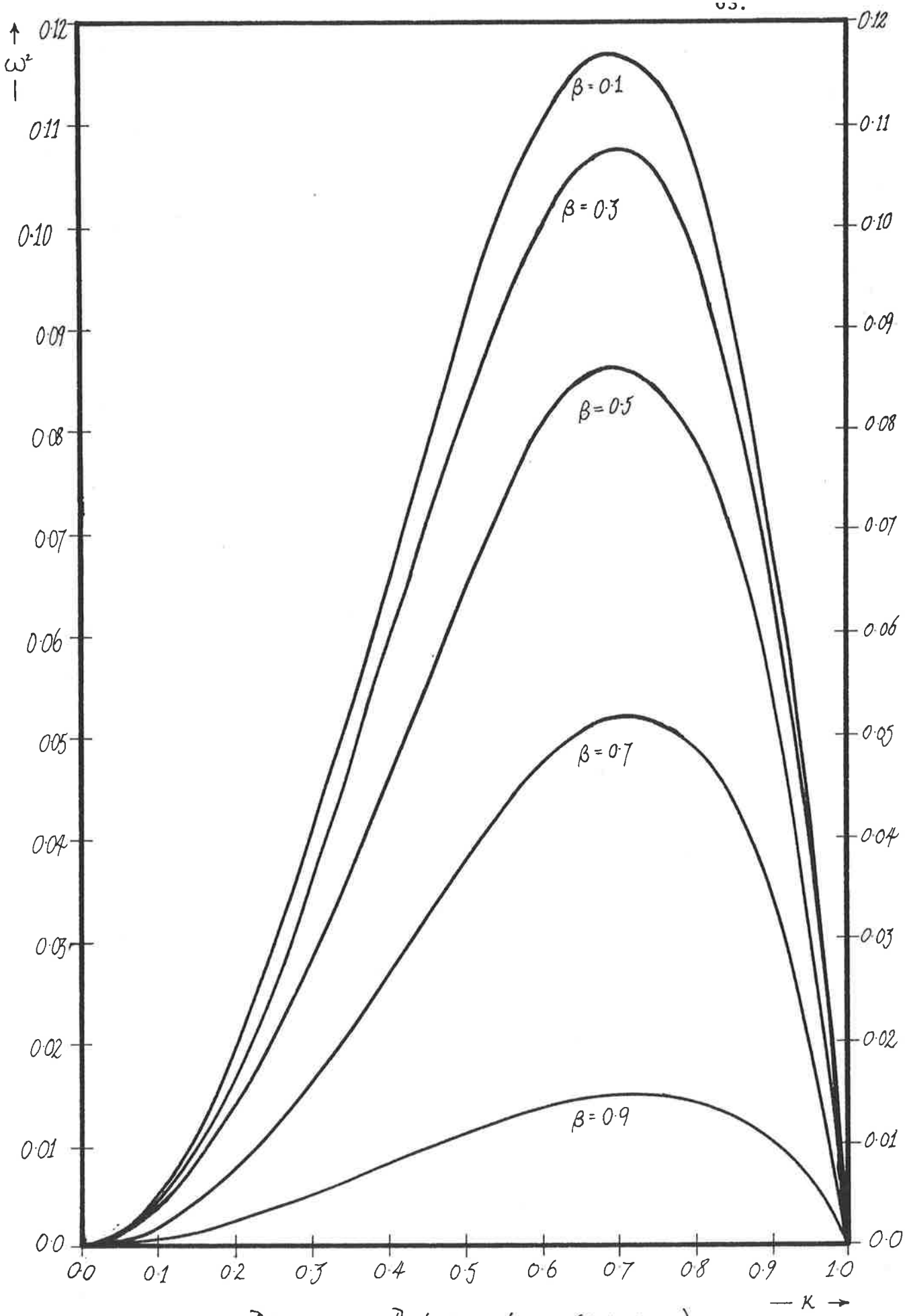

Dispersion Relationship (Mode 1.)

FIGURE 1.

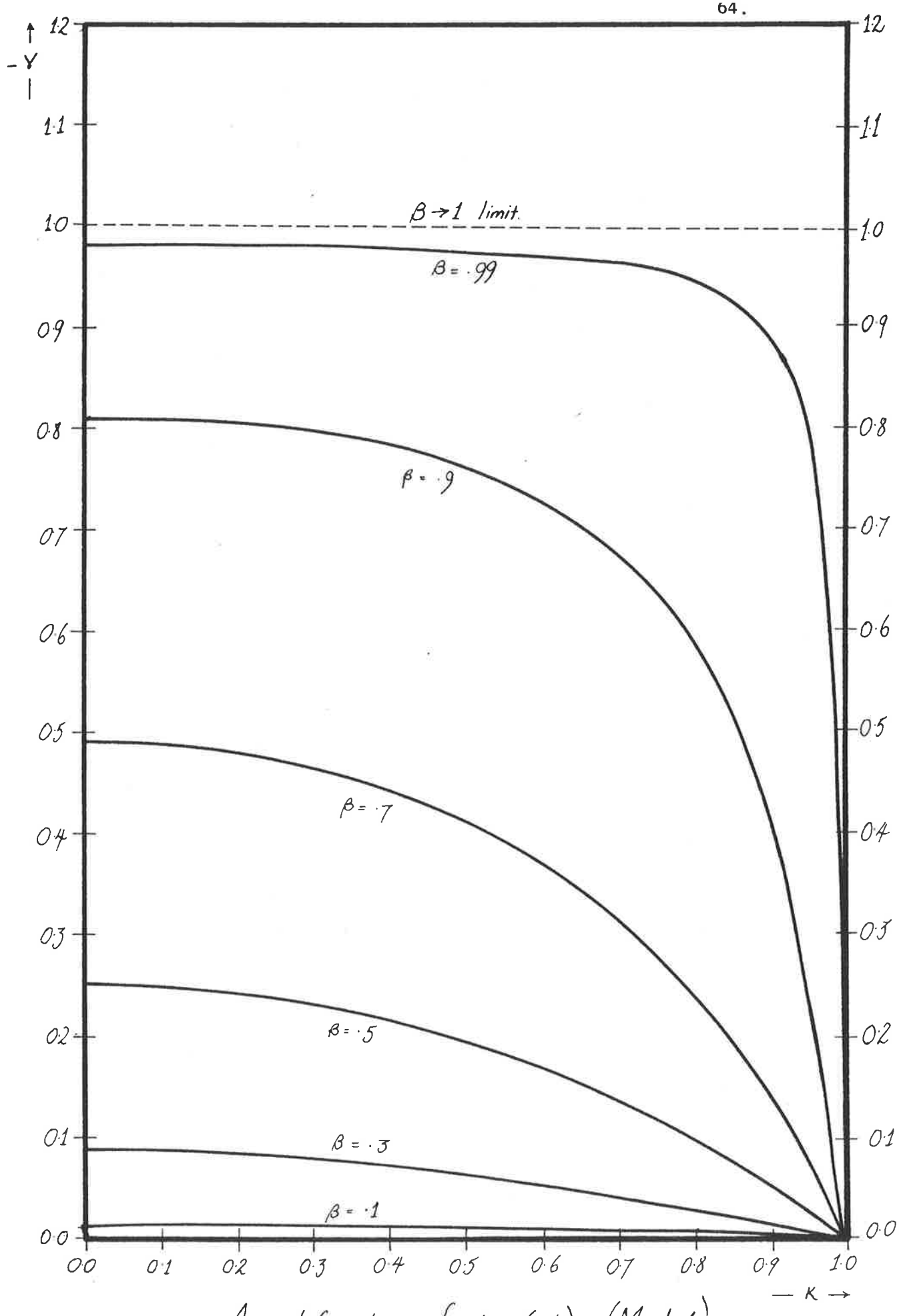

Amplification factor (Y). (Mode 1.)

FIGURE 2.

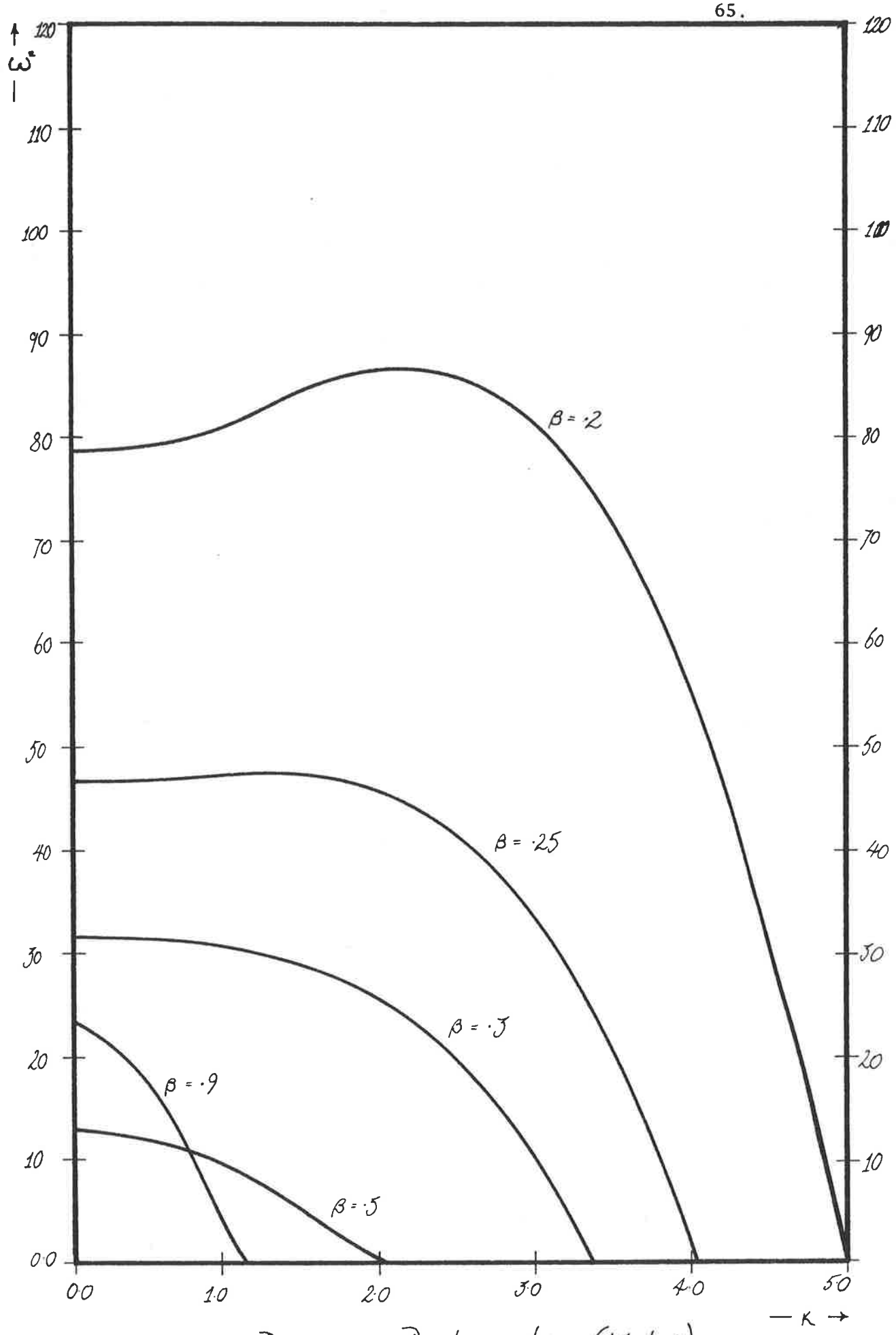

Dispersion Relationship. (Mode 2)

FIGURE 3.

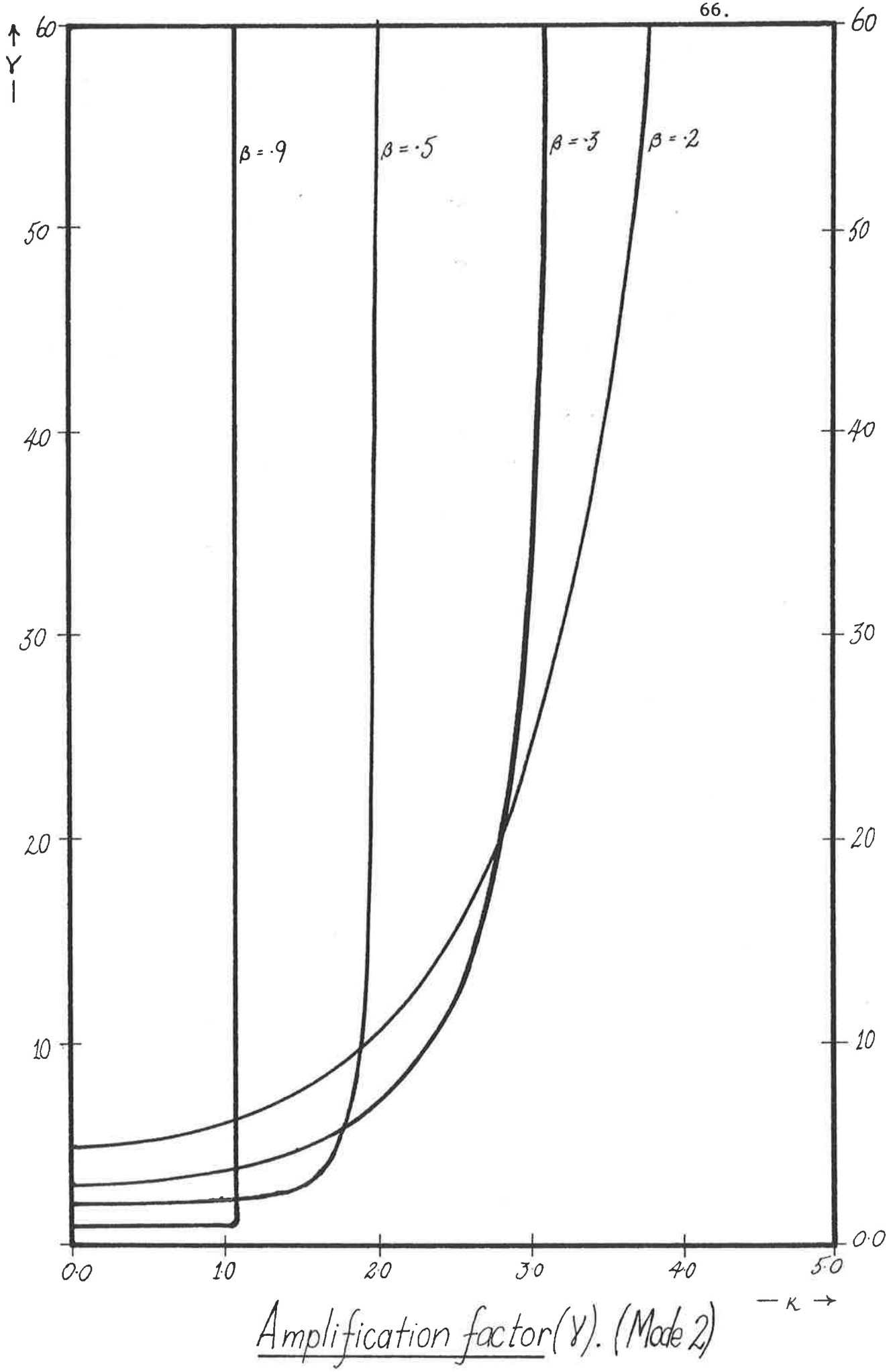

Amplification factor (Y). (Mode 2)

FIGURE 4.

however, to assume that mode-two instability, while having a far greater growth rate, is ultimately responsible for the break-up of the jet. An important case that highlights this feature is presented later.

Mode-one disturbances are only unstable for wave numbers less than 1.0. This merely states that the wavelength of the disturbance must be greater than the outer circumference. This mode bears great similarity to Rayleigh's solid-cylinder instability; indeed, the limit $\beta \to 0$, for this mode reproduces Rayleigh's solution. Figure 5 shows this clearly, and results for the maximum rate of instability, as mentioned in §2, are also shown.

It is clear however, that mode-one disturbances, by Rayleigh's maximum-mode principle, are of lesser importance than mode-two disturbances. Mode-two disturbances, while having much larger growth rates, are also unstable for much shorter wavelengths, down to $2\pi a_0$. As far as the $\beta \to 0$ limit is concerned, this is somewhat disturbing, since strictly speaking it implies that the solid cylinder (Mode-one) results are *not* recovered. Ponstein obtains two solutions to the asymptotic dispersion equation as $\beta \to 0$, namely Rayleigh's solution and another, much larger, value for the growth rate. Rather than recognize these two solutions as separate modes of instability, with quite different physical interpretations, Ponstein argues that the second, larger, solution is a spurious root, arising from the neglect of air velocities in the inner core $(r < a_0)$. While there is no doubt the neglect of air velocities in the inner core for this problem is increasingly dubious as $\beta \to 0$ the explanation we propose is far more satisfactory.

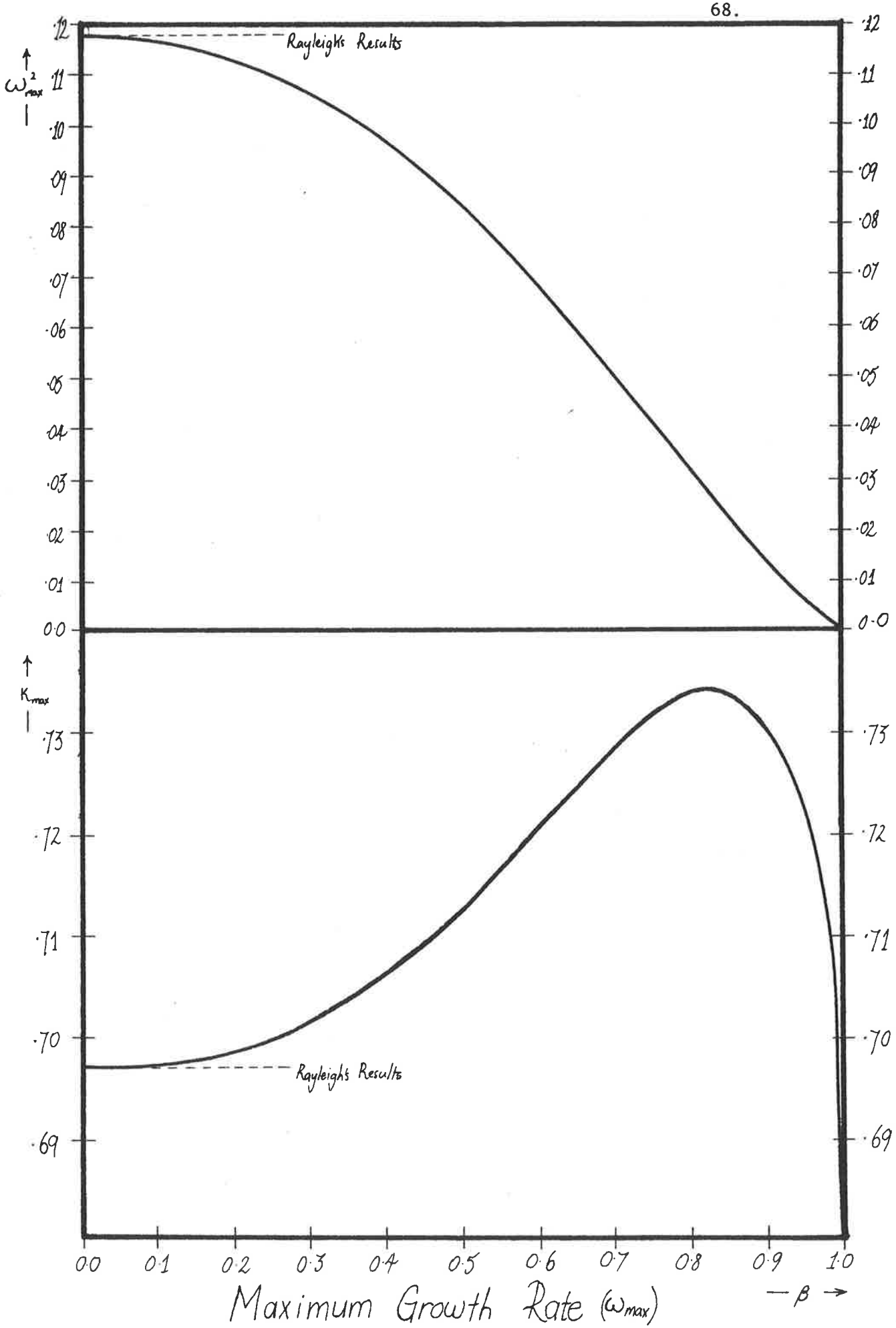

Maximum Growth Rate (ω_{max}) and Wave Number (K_{max}) (Mode 1.)

FIGURE 5.

8. SMALL β LIMIT

As $\beta \to 0$, there are two solutions to the dispersion equation. Clearly, from Figures 3 and 4 the mode-two disturbances have $\gamma \to \infty$, and except for very short wavelengths, $\sigma \to \infty$. Asymptotic formulae for these solutions, as found by Ponstein (for the growth rate) and from equation (6.9) for the amplification factor, are

$$\gamma \to \frac{I_0(\kappa)}{\beta} \quad \text{as} \quad \beta \to 0 \ , \tag{8.1}$$

and

$$\omega^2 \to -\frac{1}{\beta^3 \log\beta} \quad \text{as} \quad \beta \to 0 \ , \tag{8.2}$$

where κ is required to be in the range

$$0 << \kappa << \frac{1}{\beta} \ .$$

That is, κ is not too small and not too large. Now clearly (8.2) implies extremely large growth rates; however this does not necessarily mean a rapid break up of the jet into droplets. We must first interpret the result that γ is large, from (8.1). Given the definition of γ from (5.5) the obvious conclusion when $\gamma \to \infty$ is that $\varepsilon_2 \to 0$, which says for mode-two disturbances there is no disturbance on the outer free surface. Thus, for this mode, the oscillation of the free surface occurs *only at the inner free surface*. The rapid growth of these disturbances does not ultimately result in the jet breaking up, but rather of the inner air core disintegrating into smaller bubbles. This disturbance, even the *non-linear* fragmentation of the air core, is still only a small perturbation to the outer free surface, so the instability of the outer free surface, thus the jet as a whole is governed by the

familiar Rayleigh solid-cylinder solution.

The problem of fragmentation of the air core into smaller bubbles is analogous to the "Hollow jet" problem discussed in Chandrasekhar (1968). Furthermore, the time scale for such hollow jets is $\left(\frac{T}{\rho a_0^3}\right)^{1/2}$; thus the disparity in sizes of the growth rates for mode-one and mode-two disturbances is no more than a reflection of greatly different time scale from the hollow jet to solid jet regimes.

We now have the following physical interpretation of jet breakup, when the inner air core is small. A jet (with small β) is disturbed slightly from equilibrium; initially (and for a very short time only) mode-two dominates, and the inner air core breaks up into smaller bubbles. This whole stage is nothing but a small perturbation to the outer free surface, however it is to be expected that this perturbation is precisely the disturbance that grows, governed by the mode-one dispersion relationship, and results in the fragmentation of the jet into smaller droplets. Thus Rayleigh's results for a solid cylinder are recovered from the $\beta \to 0$ limit, provided we recognize that the inner core is only a perturbation to the jet as a whole.

A further unusual feature of the small-β limit is the instability of extremely long wavelengths, for mode-two type disturbances. This prediction is absent in the "hollow jet" theory and makes the limit a "singular perturbation" type where an alternate asymptotic solution is required for small κ. Physically it means the inner core will be highly unstable for small long range changes, for example slow variation of the ambient pressure along the jet.

In practice however, jets will not be of sufficient length to admit long wavelength instabilities.

Clearly, for small β (i.e. *thick* jets), the interpretation of modes one and two is straightforward. Another case where such distinction can be made is for very *thin* jets, that is, $\beta \to 1$.

9. THIN JET LIMITS

Equation (6.9), when considered in the limit $\beta \to 1$ produces two solutions for γ, namely $\gamma = \pm 1$. These represent two different types of waves on thin sheets, namely symmetrical and antisymmetrical, which are illustrated in Figure 6. Taylor (1959a) discussed such waves, on a *planar* sheet of liquid. Ponstein does not recognize the two forms of disturbance, but observes that thin annular sheets are extremely unstable. This is because, for anti-symmetrical waves, $\omega^2 \to \infty$ as $\beta \to 1$. Symmetrical waves on the other hand appear to be much more stable.

10. INTERMEDIATE MODES

Insight into the physical interpretation of mode-one and mode-two disturbances, away from the extreme limits of §8 and §9, is much less clear. There must now be significant interaction between disturbances on either free surface; however it is still possible to generalize the symmetric and anti-symmetric waves of §9. We see that for mode-one oscillations, γ is restricted to the range $0 > \gamma > -1$. For example, mode-one disturbances on the inner surface lag behind the mode-one disturbance on the outer surface by half a wavelength. This is analogous to the symmetrical

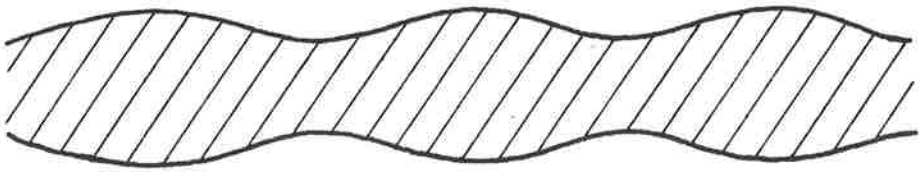

Symmetrical Waves (Mode 1) $\gamma = -1$

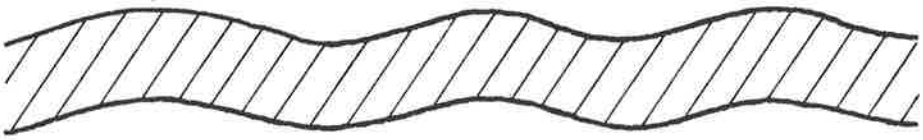

Anti-symmetrical Waves (Mode 2) $\gamma = 1$

Waves on thin Sheets of Fluid.

FIGURE 6.

waves on thin sheets. On the other hand, mode-two disturbances always have $\gamma > 0$ and thus have no phase difference across the annulus. These may be thought of as anti-symmetrical waves. The general conclusion is that anti-symmetric waves (disturbances) are much more unstable than the corresponding symmetric disturbance. This can be rationalised by recognizing that for symmetric disturbances, the mean radius of the annulus is altered by less than for anti-symmetric disturbances. This is likely to result in greater stability for symmetric disturbances.

BIBLIOGRAPHY

ABRAMOWITZ, M. and STEGUN, I.A. 1972. Handbook of Mathematical Functions. Dover.

BOUSSINESQ, J. 1869. Comptes Rendus de l'Academie des Sciences. Paris, 69, p. 128.

CHANDRASEKHAR, S. 1961. Hydrodynamic and Hydromagnetic Stability. Oxford University Press.

GEER, J.F. and KELLER, J.B. 1979. Slender Streams. J. Fluid Mech. 93, 97-115.

GILBARG, D. 1960. Jets and Cavities in Handb. der Physik, Vol. 9, 311-438. Ed. S. Flugge (Springer-Verlag, Berlin).

HOFFMAN, M.A., TAKAHASHI, R.K. and MONSON, R. 1980. Annular liquid Jet Experiments, A.S.M.E. Journal of Fluids Engineering, Vol. 102, Sept. 1980, pp. 344-349.

KELLER, J.B., RUBINOV, S.I. and TU, Y.O. 1973. Spatial Instability of a Jet, Phys. of Fluids, Vol. 16, No. 12, pp. 2052-2055.

KREYSZIG, E. 1979. Advanced Engineering Mathematics (4th edn.) New York, Wiley.

LANCE, G.N. and DELAND, E.C. 1956. The Shape of the Nappe of a Thin Waterfall. Quart. Journ. Mech. and Applied Maths., Vol. IX, Pt. 4, pp. 394-399.

LANCE, G.N. and PERRY, R.L. 1953. Water Bells. Proc. of the Physical Soc. Vol. B66, No. 397B, London, Dec. 1953, pp. 1067-1072.

PONSTEIN, J. 1959. Instability of Rotating Cylindrical Jets. Appl. Sci. Res. A, 8, pp. 425-459.

RAYLEIGH, LORD. 1945. The Theory of Sound, 2nd Edn. Dover.

TAYLOR, G.I. 1959. The Dynamics of Thin Sheets of Fluid. I. Water Bells. Proc. Roy. Soc., A, Vol. CCLIII, pp. 289-295.

TAYLOR, G.I. 1959a. The Dynamics of Thin Sheets of Fluid. II. Water Bells. Proc. Roy. Soc. A. Vol. CCLIII, pp. 296-312.

TUCK, E.O. 1982. Annular Water Jets. I.M.A. Journal of Applied Mathematics, 28, (in press).

WATSON, G.N. 1922. A Treatise on the Theory of Bessel Functions. Cambridge University Press.